CORRELATION OF THE DEPLY TECHNIQUE WITH THE ULTRASONIC IMAGING OF IMPACT DAMAGE IN GRAPHITE/EPOXY COMPOSITES*

B.T. Smith**, J.S. Heyman and A.M. Buoncristiani**
NASA Langley Research Center
Hampton, VA 23665

Earl D. Blodgett*** and J.G. Miller
Washington University
Department of Physics
St. Louis, MO 63130

S.M. Freeman
Lockheed-Georgia Company
Marietta, GA 3006

ABSTACT

The ultrasonic quantitative nondestructive evaluation (NDE) of graphite/epoxy composites is difficult due to the inherent inhomogenity of the material. An examination technique must discriminate between inherent scattering centers in an undamaged region and the scattering centers due to defects or damage. Two nondestructive techniques which can make this distinction are used to image and quantify the extent of damage resulting from a low energy impact. These results are then compared with a destructive technique. The first NDE technique, polar backscatter, employs a non-zero polar angle insonifying method to reduce specular reflection from the surface of the sample; the return signal is processed to determine the energy backscattered from a particular depth in the sample. The second NDE technique uses a normal incident ultrasonic beam; the entire backscattered wave is then signal processed to detect the presence of subsurface scatters and their respective depth in the sample. Both NDE methods are subsequently correlated with a destructive technique, the deply method. Both the qualitative and quantitative results between the methods are excellent. For the depth of material accessible by the polar backscatter method, the agreement is excellent with a correlation coefficient of 0.88 for a comparison of impact damage area determined by the deply method. A similar comparison with the signal processing method yields a correlation coefficient of 0.9.

* Work supported in part by NASA Grants: NAG-1-431 and NAG-1-1601.

** Christopher Newport College, Physics Dept. Newport News, VA

*** present address: University of Wisconsin-River Falls, WI

INTRODUCTION

The nondestructive detection and evaluation of impact damage in structures fabricated from graphite/epoxy composite material is important to the use of these materials in the aerospace industry. Low energy impacts on these materials will typically leave no visual damage at the impact site, but can result in internal damage. The objective of the work presented here is to demonstrate quantitative NDE techniques for assessment of impact damage in graphite/epoxy composite by comparison with a quantitative destructive measurement. Portions of this work have been previously reported [1,2].

One approach to the nondestructive evaluation of inherently inhomogeneous materials makes use of quantitative images based on ultrasonic backscatter[3]. A typical pulse-echo measurement is performed with the insonifying beam incident perpendicular to the specimen surface (a polar angle of zero degrees). Perpendicular insonification in an immersion measurement system results in a large specular reflection due to the acoustic impedance mismatch at the fluid/composite interface. This specular reflection may dominate the ultrasound backscattered from features of interest within the specimen. We note that effects of the large specular reflection on the backscattered signal can be significantly reduced by insonifying at non-perpendicular incidence (i.e., at a non-zero polar angle). An early application of this technique was used by Brown [4] in an investigation of the effects of fatigue in carbon fiber reinforced plastics. Brown's "dark-field" technique of insonifying at a non-zero polar angle was motivated by some observations on scattering by Bhatia[5]. A significant extension of the "dark-field" technique for anisotropic or quasi-isotropic materials such as fiber reinforced composites was independently introduced by Bar-Cohen and Crane[6]. This "polar backscatter" technique uses the fact that signals from cylindrical structures such as fibers are maximum when the insonifying beam is perpendicular to the long axis of the fiber, and falls substantially as the angle of insonification changes from perpendicular. Thus, the backscatter at a fixed polar angle exhibits a distinct, systematic azimuthal variation, with sharp peaks in backscatter that occur where the insonifying beam is perpendicular to any of

the principal fiber orientations in the composite.

In a previous paper from the Washington University group[7], quantitative images of polar backscatter were used to investigate impact and fatigue damage in thin graphite fiber reinforced laminates. In that study, images of polar backscatter were obtained with the azimuthal angle of insonification perpendicular to each of the four fiber directions present, so that each image was selectively sensitive to scatterers (fibers and damage) oriented along the specific fiber directions. The results suggest that low velocity impact results in more damage in laminae furthest from the side impacted, with damage in a specific lamina oriented along the fibers in that lamina. The findings presented here will further confirm these earlier investigations.

Another approach to the nondestructive evaluation of composites involves the acquisition of the entire ultrasonic wave that is backscattered from the sample. The basic approach is similar to the pulse-echo measurement performed in a liquid bath. In the usual method the received wave is pre-processed to measure the group velocity, magnitude, or frequency content and a single number is retained to describe the response of the material at that location. In contrast, the method employed here digitizes the entire backscattered wave so as to include the front, internal and back surface reflections. The digitized wave form is stored for post-processing. The data contains all the information necessary to calculate the usual parameters such as attenuation and velocity. In addition using signal processing techniques the internal scatterers in the material can be detected and displayed. The aspect of the work presented here will concentrate on the quantitative determination of the internal scatterers as a function of depth in the material.

The destructive evaluation technique known as deply, developed by one of the authors, S.M. Freeman(6), permits the characterization of impact damage at every interlaminar interface. In this technique the impact zone is saturated with a solution of AuCl, which penetrates into the regions of matrix cracking and delaminations formed by the impact. The composite is then heated to partially pyrolyze the resin matrix and thus allow the lamina by lamina separation of the laminate. The damage at each interface is highlighted by

gold left at the damage site. This allows the characterization of the area, orientation, and shape of the damage as a function of depth. The types of damage that can be imaged by this method include delaminations, fiber fracture and matrix cracking. The work presented here will concentrate on quantitative imaging of impact generated delaminations.

The samples examined were fabricated and impacted at Lockheed-Georgia. They were subsequently sent to NASA Langley for the digitization procedure and to Washington University for the polar backscatter ultrasonic inspection. Following the nondestructive evaluation they were returned to Lockheed-Georgia for the deply inspection procedure. In this report, the impact samples will be described first followed by the results of the deply procedure. The polar backscatter technique will be presented next, followed by the results of the digitization technique. Included in each ultrasonic section is the comparison between the destructive and nondestructive techniques.

IMPACT SAMPLES

Two test panels, 6.0 x 10.0 inches, were removed from a 16-ply graphite/epoxy laminate fabricated from Hercules AS4/3502 prepreg tape. The stacking sequence for this laminate was

$$[0°/^{+}45°/-45°/90_2°/-45°/^{+}45°/0°]_s$$

and consisted of 13 laminae with a possibility of 12 locations for InterLaminar Delamination (ILL). A lamina is defined as contiguous and similar ply orientations. The panels were ultrasonically 'C' scanned to verify the absence of damage before impacting.

The panels were mounted in a special test fixture that provided vertical boundary supports spaced 3.0 inches apart. Two sites were impacted on each panel using a 0.5 inch diameter aluminum ball fired from a compressed air gun at a velocity of 150 feet per second. The end of the gun barrel was positioned 5 inches from the panel surface. Ball velocity was measured by two sensors spaced 6 inches apart on the gun barrel. For each panel both impact sites were between the same vertical boundary supports. The impacted side

will be identified as the front surface for the purposes of clarity in the analysis. The impact sites were subsequently subjected to TBE (tetrabromoethane) enhanced x-ray radiography to verify that damage was present. The panels were then baked at 150F for 2 hours to remove the TBE.

Destructive Characterization Method: Deply

The deply inspection procedure consists of the application of a matrix damage marker solution to the graphite-epoxy panel followed by a partial pyrolysis of the resin matrix, unstacking the laminae, examination of the laminae, and damage or defect quantification.

Application of Marker Solution

A solution of gold chloride in diethyl ether (9.0% by weight gold) was applied to the composite face opposite the point of impact. There must be a pathway, even microscopic, that connects the damage area to the surface or edge of the composite to allow penetration of the marker solution. A dam of vacuum bag putty, with a mylar cover was used to keep the solution in contact with the composite for about 60 minutes. Following the soak interval, the excess gold solution was removed and saved for recycling. The panels were heated to approximately 150F to remove the solvent before proceeding with the pyrolysis.

Pyrolysis

Segments of the graphite-epoxy composite containing the impact damage were placed on a stainless steel wire mesh holder and inserted into a zone of a tube furnace maintained at 785F for 70 to 100 minutes. Following completion of the pyrolysis period the segments were removed from the furnace and allowed to cool. All segments were sufficiently pyrolyzed after 90 minutes to be suitable for unstacking.

Unstacking

The segments were carefully removed from the holder and placed on a work table. Each lamina of a segment was reinforced with transparent tape, lifted from the the segment and stored in a small container. Normally the laminae are mounted on a worksheet with a piece of double-coated tape; however, these laminae were left unmounted to facilitate damage quantification. When unstacked in this manner the laminae were "flipped" so that the surface for observations was that of the "bottom surface" of the lamina just removed, or expressed in another way, the view was that of the "top half" of the interlaminar location. If one compares the gold marked area on the "bottom surface" of the lamina just removed with the gold marked area on the "top surface" of the remaining segment one observes that one area is mirror image of the other. Care was exercised at this point to avoid touching the exposed surface of the lamina, as this will sometimes blur the very small matrix crack indications that can be just a fraction of a millimeter in width and not readily apparent to the unaided eye. Figure 1 shows a typical view of gold marked impact damage.

Examination of Laminae

The most important requirement for observing the surface of a lamina for fiber-bundle fracture, matrix cracking indications and delaminations is proper illumination. Of course, some of the gross damage indications can be seen with makeshift lighting, but not the finer details. Fiber fracture is best observed with fluorescent light impinging at 90 degrees to the fiber direction. The optimum illumination for gold chloride marked matrix damage is a high intensity light impinging on the lamina surface parallel to the fiber direction. For observing fiber-bundle fracture, small areas of delamination, and matrix cracking indications, a binocular microscope with a magnification range of approximately 7X to 50X is ideal.

Damage Quantification

The area of delamination for each interlaminar location at each impact site was determined with an image analyzer using a macro-viewer lens. The orientation of the damage with respect to adjacent fiber orientation will be discussed in the next sections. The distribution of the delamination sizes through the thickness of the laminate can be readily visualized when the deply determined area for a single impact site versus interlaminar location is presented in a histogram format in figure 2. Interlaminar location 1 on the histogram is adjacent to the impacted (front) side of the panel. Also included in the figure is the ply orientation of the corresponding lamina.

The trend of increased damage opposite the impacted face has been previously reported [7,8,13]. In thin flexible plates such as the specimens in this study, this trend has been interpreted in terms of plate bending stesses[14]. Thicker less flexible composite laminates may exhibit local subsurface damage more proximal to the impacted face[14].

Nondestructive Characterization Method: Polar Backscatter

Each of the four impact sites was investigated using the polar backscatter technique. The experimental procedure was similar to that used in a previous study[7]. Four scans were obtained of each impact site. The scans corresponded to selective interrogations perpendicular to each of the four fiber orientations present in these samples. The panel being investigated was mounted on a motorized platform immersed in a water bath, with the back surface facing the interrogating transducer. The (polar) angle of incidence was chosen to be 30° for all scans in this work. This polar angle is greater than the critical angle for quasi-longitudinal wave transmission into an anisotropic half-space for any azimuthal angle of incidence as determined from slowness surfaces based on the elastic constants for graphite-epoxy[9-11]. Consequently, interrogation of regions of damage interior to the specimen is expected to occur with quasi-shear waves. The azimuthal angle of the interrogating transducer was adjusted to be

perpendicular to the selected fiber orientation of each scan.

A 0.5 inch diameter, 4 inch focal length broadband transducer, nominally centered at 5 MHz, was used in pulse-echo mode as the interrogating transducer. Approximately eight microseconds of backscatter from the sample were gated into an analog spectrum analyzer. The received spectrum at 288 frequencies over the range 2 to 8 MHz was averaged and normalized to the frequency average of the spectrum reflected from a flat stainless steel plate. Thus the numerical values of the polar backscatter reported here represent a quantitative measure of the broadband response of the interrogated material. The broadband frequency average of the backscatter reduces errors due to interference effects in the ultrasonic field and phase cancellation at the piezoelectric element of the transducer[3,12].

Each scan was 6.1 cm. by 6.1 cm. corresponding to 61 by 61 measurement locations with a spacing of 1 mm. The impact site was approximately centered in the region to be scanned.

Data Reduction

The ultrasonic information contained in the polar backscatter scans was cast into gray scale image format. Examination of gray scale images provides qualitative information regarding the shape and orientation of damage structures. An example of a gray scale image based on quantitative polar backscatter is presented in figure 3. The image in figure 3 is based on a polar backscatter scan of one impact site with the interrogating beam perpendicular to the +45° fiber orientation. (We note that the scan was performed from the back resulting in an apparent reversal of the +45° and -45° directions.) The discrimination levels for the gray scale were chosen so that there are 16 equally spaced gray levels. The lightest level corresponds to backscatter less than -42.0 dB below that from a near perfect reflector, the darkest level to backscatter greater than -30.0 dB below that from a nearly perfect reflector. Although the damage is evident, the exact boundary of the damage zone is blurred by the beam width of the interrogating beam, which is

several pixels wide at low frequencies.

Because the choice of discriminant levels can affect the qualitative aspects of a gray scale image, quantitative estimation of the area of damage based on a visual impression obtained from a gray scale image is often inaccurate. We have chosen a method which provides an unbiased estimate of the area of damage, based on the distributions of the measured polar backscatter values for undamaged and damaged zones. The damaged area shown in figure 3 is characterized by stronger scattering than the nominally undamaged regions. Figure 4 represents a histogram of the distribution of the polar backscatter displayed in the region of figure 3. The higher scattering values corresponding to the zones of damage can be seen as the "tail" extending from approximately -37 dB. The area of damage is a small fraction of the total image area, so that most of the histogram represents the distribution of backscatter from essentially undamaged regions. We chose to approximate this background by a normal distribution, which was determined by least-squares techniques. The smooth dark line in figure 4 was generated from the least-squares parameters of the background distribution. An estimate of the area of damage was obtained by integrating the high scattering "tail" of the histogram and subtracting off the integral of the background distribution calculated over the same range of backscatter.

The apparent area of damage was determined by this histogram subtraction technique for all 16 images. The histogram information was also used to select appropriate threshold levels for the generation of the bi-stable gray level images shown in figures 5 and 6. The choice of a bi-stable display was made to simplify comparison with the photographs of damage obtained by the deply technique. In each image, the darker level represents higher scatter, starting at the (approximate) lowest values corresponding to scatter from damage, as determined from the histogram information.

Correlation of Results

The polar backscatter measurements represent a superposition of scattering from damage in several similarly oriented layers, with attenuation from

intervening layers reducing the contributions from deeper layers. The deply technique provides information on damage at each interlaminar interface. We chose a subset of the deply technique information appropriate for correlation with the polar backscatter technique. Because we are testing the hypothesis that the polar backscatter technique is selectively sensitive to damage structures which are oriented perpendicular to the interrogating beam, the orientation of damage is the primary selection criterion for correlation. As an example, the polar backscatter scan of figure 3 clearly indicates damage oriented in the +45° direction, as expected from the angle of interrogation. This polar backscatter scan should therefore be correlated with interlaminar locations which the deply technique indicates has damaged zones oriented in the +45° direction. Inspection of figure 2 reveals four interlaminar locations which exhibit this damage orientation: locations 1,5,7, and 11. Although one might initially envision the superposition of the damage zones in these four interlaminar locations as the damage zone which could be correlated with the polar backscatter technique, further consideration suggests that superposition may not be appropriate. The attenuation of quasi-shear waves in graphite-epoxy laminates can be substantial. Previous work from this laboratory[7] has shown that the polar backscatter technique in similar composite laminates is primarily sensitive to structures nearer the insonified surface. Thus, signals from damage farthest from the insonified surface such as that in interlaminar location 1 will be significantly attenuated. We also note that qualitative superposition of similarly oriented damage zones suggests that the zones overlap to a significant extent, so that the largest damage zone provides a good estimate of the superposition. Combining these two considerations with the fact that we interrogated from the back surface where damage is more extensive led us to the following simple correlation criterion. The polar backscatter scan of a given orientation was correlated with the deply information from the interlaminar location exhibiting the largest area of similarly oriented damage, as indicated in figure 2. Specifically, we chose to correlate the deply information from interlaminar location 11 with the +45° polar backscatter image, interlaminar location 8 with the -45° polar backscattter , interlaminar location 9 with the 90° polar backscatter, and interlaminar

location 12 with the 0° polar backscatter.

The approximate size, shape and orientation of damage is qualitatively correlated in figures 5 and 6. The area represented by each image in these figures is approximately 2.6 cm. by 3.7 cm. The scaling allows direct comparison between polar backscatter images and deply photographs.

The left panel of figure 5 presents the polar backscatter image obtained with the interrogating ultrasound perpendicular to +45° fiber orientation. The right panel presents the corresponding deply photograph from interlaminar location 11 of that impact site. The damage visualized by both techniques is clearly oriented along the +45° direction, as defined from the top of the sample. (Both of these evaluation techniques are examining the specimen from the bottom, so that the +45° and the -45° orientations appear to be exchanged.) The shape and extent of damage in each panel are in good qualitative agreement.

Figure 6 presents the three remaining orientations for this impact site. The top panels present the results of interrogating perpendicular to the -45° orientation and the corresponding deply photograph from interlaminar 9, and the lower panels 0 ° and the interlaminar location 12. There is good qualitative agreement between polar backscatter and deply for the orientation, size, and general shape of the damaged regions.

A quantitative correlation of these techniques can be obtained from the estimates of area. Figure 7 presents a correlation plot of the damage area as determined by polar backscatter versus the damage area determined by the deply technique. The linear correlation coefficient, calculated by including the error estimates shown in figure 7 is r=0.88.

In summary, the size, shape, and orientation of damage correlates well between the polar backscatter technique and the deply technique. Further, there is good quantitative correlation between the areas of damage indicated

by the two techniques. These results suggest that the polar backscatter technique is sensitive to specific orientations of damage. The polar backscatter technique provides a good qualitative image of the size and shape of the largest zone of damage in each of the principal orientations. A quantitative estimate of the extent of these largest damage zones can be obtained from the polar backscatter technique. The selective sensitivity of polar backscatter may thus provide a useful tool for further studies of the mechanisms of impact damage in graphite-fiber reinforced composite laminates.

Nondestructive Method: Digitization and Signal Analysis

In contrast to the previous section where the polar backscattered wave was gated into a spectrum analyzer, in this procedure the entire normally incident wave is digitized and stored. The entire waveform describes the sample response at each location. Conventional C-scan techniques provide a single value integrated through the thickness of the material response at a location. The digital record, on the other hand, determines the material response for the full three dimensions of the sample. To analyze the data, signal processing techniques are applied to the digital record to develop an image from the backscatter signal from impact generated delaminations as a function of their depth in the material. A description of the experimental procedure will be followed by details of the signal processing, data reduction and a comparison with the deply method.

The experimental technique involves digitizing the entire backscattered wave from the sample. A focused damped transducer with a center frequency of 15 MHz was used as both the transmitter and receiver. A single cycle of a 15 MHz sine wave is used to excite the transducer. The experiment is performed in a water bath and the backscattered wave is acquired at 200 megasamples per second with an eight bit digitizer so as to include the front, internal and back surface reflections from the sample in a time record of 1024 channels. The transducer, held at normal incidence, is stepped in an x-y pattern over an area of 4 x 4 centimeters with a 2 millimeter stepsize which is on the order of the beam spread. The entire scan takes approximately 15 minutes to complete. This procedure is followed for waves incident on both the impacted

and back side of the specimens. The data is stored in a computer in the form of a 3 dimensional array of x-y and time. In later analysis this will allow examination of a particular depth in the sample by sectioning the array at the time corresponding to that depth.

Shown in figure 8a is a typical backscatter signal from an undamaged region of the composite. The signal is plotted as relative amplitude versus time in units of 5 nS. The front (channel 200) and back (channel 500) surface reflections are quite evident. Further processing of this signal is necessary to delineate the subsurface damage which contributes that portion of the signal that is contained between the front and back surface reflections. The object of the signal processing is to determine the material response to the ultrasonic wave. The returned signal is a function of the material response and the input signal. This is shown schematically:

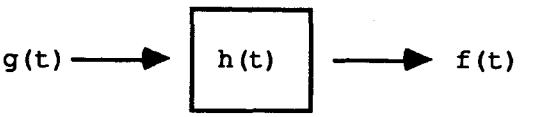

where g(t) is the input function, h(t) is the transfer function for the material and f(t) is the measured response. The functional relationship for a linear time invariant system is given by:

$$f(t)=\int h(t-t')\ g(t')\ dt'.$$

This convolution of the input signal and material response leads to the observed signal. The material response independent of the input signal and system response is the quantity of interest in evaluating the material. To achieve this result, the integral equation can be solved by Fourier transform techniques[15]. The properties of Fourier transforms allows one to rewrite the equation in terms of the frequency space Fourier transforms as a product:

$$f(\omega)=g(\omega)*h(\omega).$$

Now calculating the reciprocal of $g(\omega)$ the material response in frequency space can be determined.

$$h(\omega)=f(\omega)/g(\omega)$$

Taking the inverse Fourier transform of this ratio provides the deconvolved material response in the time domain. Before taking the inverse Fourier transform of $h(\omega)$ the result is filtered to remove least significant bit noise in the data which results in unwanted high frequency noise contributions. The filter employed in this analysis was a band pass filter with unit gain from 5 to 20 MHz and with side wings that rolled off as a cosine function for 0.5 MHz on each side. The Fourier transforms are all determined by numerical Fast Fourier Transform techniques. Implicit in the input function is the response of the total system as well as the input wave form. The system response is determined by measuring the reflection from an ideal reflector which in this case is an aluminum block. The impedance difference between aluminum and the composite was not used to renormalize the system response since we are only interested in relative differences between damaged and undamaged material. The system response which corresponds to $g(t)$ is shown in figure 8b and the result of the deconvolution is shown in figure 8c. From the display in figure 8c the presence of subsurface scatterers is quite evident as compared to the raw data of figure 8a.

To more accurately locate these scatterers in time and thus depth another level of signal processing is necessary. The output of the deconvolution procedure is used as the input to a calculation of the analytic function and finally its magnitude. The magnitude of the analytic function has been shown to be equal to the rate of arrival of the energy of the wave [16]. It should be noted that the energy as measured here is for the as received wave and does not correct for phase cancellation effects at the face of the transducer. The form of the analytic function for the backscattered ultrasonic wave is determined by taking the Hilbert transform of the deconvolution $h(t)$. This provides the imaginary part of the analytic

function. The full complex analytic function can be written as:

$$h_A(t)=h(t) + i\ H[h(t)]$$

where h(t) is the result of the deconvolution and H[h(t)] is the Hilbert transform of the signal.

$$H[h(x)] = \frac{1}{\pi}\int_{-\infty}^{\infty}\frac{h(x')\ dx'}{x'-x}$$

The Hilbert transform is equivalent to the convolution of the signal with the kernel $1/(\pi t)$ and techniques for calculating the analytic function from the original signal are well documented [17]. Using complex Fourier transforms the material response in time space is Fourier transformed to frequency space where all the negative frequencies are zeroed before taking the inverse Fourier transform. This result is equivalent to the analytic form of the signal. The magnitude of the analytic function is then formed from the square root of the sum of the squares of the real and imaginary parts of the function.

The results from this two step signal processing are seen in figures 9a for an undamaged and 9b for a damaged composite. The record of figure 9a is the result of calculating the magnitude of the analytic function determined from the result of the deconvolution shown in figure 8c. The advantages to this result are that now scatterers are well localized in time and thus depth, also the signal is unipolar which will facilitate easy interpretation of the data. The large subsurface scatter in figure 9b at channel 480 is well evident and corresponds to a signal from a delamination at ILL 5 within the sample (the shift in time scale from that of the observed signal is an artifact of the signal processing). A signal at the same location in time is also evident in figure 9a. In the same manner the other internal scattering peaks in figure 9a can be identified in relation to the ply locations of the sample. The numbers indentifying the peaks correspond to the probable interlaminar locations. Thus, this analysis

resolves not only subsurface scatterers but may also resolve individual lamina in an undamaged material. The following discussion concentrates on imaging impact delamination damage.

Although the damage at one x-y location is readily identified in figure 9b ,it would be quite tedious to examine all 400 records manually and cross correlate signal strength with depth to provide a three dimensional view of the impact damage. A method which can dynamically provide this analysis has been developed with the use of a image analyzer. The image analyzer displays a two dimensional array of pixels on a raster type CRT. Each pixel in the array is scaled over 8 bits giving a range of values from 0 to 255 which are displayed as shades of gray. This mode of display is quite common for C-scans where each sample position is designated by a value of the relative attenuation at that point scaled by the bit resolution of the image analyzer. The analyzed signal forms a three dimensional array in x-y and time and the image analyzer provides a means of dynamically viewing this data. Time slices are taken of the array for each channel (5 nS per channel which equals 0.0165 mm) and each slice is a 20x20 array of the amplitude of the processed signal at that channel (depth). The slices in time and thus depth are displayed sequentially on the image analyzer at any speed per frame that is convenient. These frames form a movie in time which is equivalent to viewing the backscatter from the composite in pseudo real time as if one where "flying" through the composite. This movie can be frozen or run forward and backward in time.

A criterion for determining the total damage at each frame and thus depth can be identified. Since the transducer was kept parallel to the composite, the relative phase between scatterers at the same depth is approximately zero and a well imaged backscatter return for damage is well above the background scatters such as the individual plys. This is illustrated here by a comparison of figures 9a and 9b. The size of the scatterer identified at channel 480 in figure 9b is well above the corresponding scattering signal at channel 480 in figure 9a. We arrive at an estimate of the damage area as a function of depth in the material by processing the data to image just the damage of interest. The area of the

damage at each depth is much less than the entire frame area so that the image distribution is centered about the average background value of scatterers. The backscatter from delaminations is well above this background level. A statistical analysis of each frame is a means of determining the total area of damage. This was accomplished by calculating the standard deviation of the amplitude distribution of the entire 20x20 array for each frame in the movie. Shown in figure 10 is the distribution of scattering amplitudes for the entire frame and a subsampled region which contains no impact delaminations. The distribution for an entire frame is seen to extend to large values whereas the undamaged region exhibits a sharp cutoff. For the purpose of this analysis a standard 2σ greater than the median value (μ) of the distribution was taken as the lower limit for inclusion in the damage area. These values are indicated on the graph. Thus for each frame every pixel value that was greater or equal to $\mu+2\sigma$ was included in the damage area calculation for that frame. This criterion is conservative and for an automatic testing procedure optimization of the cut off value would be of interest.

Shown in figure 11 is the comparison between the deply results and the ultrasonic results for one of the impact samples with all 12 possible interlaminar locations. The top label corresponds to the intelaminar location. The ultrasonic data is from the frame that corresponds to the same depth for the deply data. The gray scale images, figure 11a, have been highlighted to show the area which meets the statistical criterion, while the three dimensional wire plots, figure 11c, illustrate the relative signal to noise contained in the gray scale display of figure 11a before clipping. The deply results for the same ILL is shown in figure 11b. The data for ILL 7 through 12 is from interrogation of the back side of the sample.

Correlation of Results

A comparison of the delamination area determined by the deply and ultrasonic techniques is shown in figures 12 and 13. The data for all four

impact points and all possible (12 for each sample) interlaminar locations are included in these plots. The line shown in figure 13 is a least square fit to the data with a correlation coefficient of 0.90. The data suggest a trend related to the measurement technique. The front locations one through three tend to larger values for the ultrasonic technique than the deply technique. This discrepancy may be due to actual larger damage area that because of lack of microscopic channels the gold chloride solution did not penetrate. The explanation may also be in the fact that it is difficult to resolve the backscatter from the first ILL and the front surface (this also applies to ILL 12). The ILL of four through eleven tend to lower ultrasonic determined areas then the deply measurement. This is due mainly to shadowing of underlying delaminations by preceding damage. A comparison of gold chloride data of figure 11b. with that of the wire plots of figure 11c and the gray scale images of figure 11a shows that whereas, there is central damage in each layer shown, the ultrasonic data shows no backscatter signal in the central region. This shadowing tends to lead to an underestimation of total damage area.

In summary, the correlation between the two techniques can be considered very good both qualitatively and quantitatively. The data reveals a characteristic dumbbell shape that is very evident in the deply data as well as the gray scale of the magnitude of the analytic function from ultrasonic inspection (figure 11). These shapes have an axis of symmetry coaxial with fiber direction of the underlying lamina (away from the direction of impact) at the interlaminar location. In the movie format viewed at a few frames per second the shapes are easily resolved and their shift with fiber orientation is easily observed. Lastly, the technique can provide through the thickness information on the ply lay-up and damage.

Conclusion

The two ultrasonic techniques both exhibit advantages in their respective uses. The polar backscatter technique is very sensitive to the ply orientation, and has use in not only damage detection but verification

of ply layup. The digitization technique provides through the thickness damage information and the spacing between lamina in undamaged regions. In conclusion, we have presented nondestructive evaluation techniques which are in good quantitative agreement with an exact destructive technique. The ultrasonic methods provide through the thickness information on damage and require access to a single side of the material. The deply technique though destructive gives exact information on the actual damage and is important as a tool for understanding the impact damage dynamics.

REFERENCES

1. Blodgett, Earl D., S.M. Freeman, and J.G. Miller,"Correlation of Ultrasonic Polar Backscatter with the Deply Technique for Assessment of Impact Damage in Composite Laminates", Review of Progress in Quantitative Nondestructive Evaluation, vol. 5, pp 1227-1238, (1985).

2. Smith, B.T., J.S. Heyman, J.G. Moore, and S.J. Cucura,"Correlation of the Deply Technique with the Ultrasonic Imaging ot Impact Damage in Graphite/Epoxy Composites", Review of Progess in Quantitative Nondestructive Evaluation, vol. 5, pp 1239-1244, (1985);
Smith, B.T.,A.M. Buoncristiani,"Digital Signal Processing Methods for Ultrasonic Backscattered Waves in Composite Materials", IEEE 1986 Ultrasonics Symposium Proceedings, Williamsburg VA, November 1986, to be published.

3. O'Donnell, M., J.G. Miller,"Quantitative Broadband Ultrasonic Backscatter: An Approach to Nondestructive Evaluation in Acoustically Inhomogenous Materials", Journal of Applied Physics, vol. 52, pp. 1056-1065, (1981).

4. Brown, A.F. ,"Materials Testing by Ultrasonic Spectroscopy", Ultransonics, vol. 11, pp 202-210, (1973).

5. Bhatia, A.B. ,"Scattering of High-Frequency Sound Waves in Polycrystalline Materials" ,Journal of Acoustical Society of America, vol. 31, pp 16-23, (1959).

6. Bar-Cohen Y.,R.L. Crane,"Acoustic-Backscattering Imaging of Sub-critical Flaws in Composites", Materials Evaluation, vol. 40, pp 970-975, (1982).

7. Thomas III, L.J., E.I. Madaras, and J.G. Miller,"two-Dimensional Imaging of Selected Ply Orientations in Quasi-Isotropic Composite Laminates Using Polar Backscattering", IEEE Ultrasonics Symposium Proceedings,vol 82 CH 1823-4, pp965-970, (1982).

8. Freeman, S.M. ,"Correlation of X-Ray Radiograph Images with Actual Damage in Graphite-Epoxy Composites by the Deply Technique", Composites in Manufacturing 3 Conference, vol. EM84-101, pp 1-13, Society of Manufacturing Engineers, Dearborn, Michigan, (1984).

9. Thomas III, L.J., "Ultrasonic Backscatter: A Quantitative Index of the Elastic Properties of Inherently Inhomogeneous Media", PhD Thesis, Washington University, St. Louis, Mo., (1985)

10. Auld, B.A., Acoustic Fields and Waves in Solids, Vol. 1, Wiley Interscience, New York, (1973).

11. Kriz, R.D., W.W. Stinchcomb,"Elastic Moduli of Transversely Isotropic Graphite Fibers and Their Composites",Experimental Mechanics, vol. 19, pp 41-49, (1979).

12. Busse, L.J.,J.G. Miller,"Detection of Spatially Nonuniform Ultrasonic Radiation with Phase Sensitive (Piezoelectric) and Phase Insensitive (Acoustoelectric) Receivers",Journal of Acoustical Society of America, vol. 70, pp 1377-1386, (1981).

13. Chai, H. , W.G. Knauss, and C.D. Babcock,"Observation of Damage Growth in Compressively Loaded Laminates", Experimental Mechanics, vol. 23, pp 329-337, (1983).

14. Zukas, J.A., T. Nicholas, H.F. Swift, L.B. Greszczuk, and D.R. Curran, Impact Dynamics, John Wiley & Sons, New York, (1982).

15. Bracewell, R.N. , The Fourier Transform and Its Appication, McGraw-Hill, New York, (1982).

16. Heyser, R.C. ,"Determination of Loudspeaker Signal Arrival Times Part III", Journal of the Audio Engineering Society, vol. 19, pp 902-905, (1971).

17. Gammell, P.M. ,"Improved Ultrasonic Detection Using the Analytic Signal Magnitude", Ultrasonics, vol. 19, pp 73-76, (1981).

FIGURE CAPTIONS

1. Example of photograph of the gold deposited at a damage site.

2. Area of damage at the interlaminar locations. The underlying ply orientation is noted. The impacted surface is adjacent to ILL 1.

3. Example of a gray scale image of a full 61 mm by 61 mm polar backscatter scan, interrogating perpendicular to the +45° orientation. The damage structure is oriented along the +45° direction.

4. Histogram of the quantitative backscatter values from the polar backscatter scan presented in figure 3. The bin size was 0.1 dB. The heavy smooth line represents a normal distribution fit to the background.

5. Comparison of apparent zones of damage imaged by the polar backscatter technique (left panel) with the photograph of damage indication from the deply technique. Orientation fo the damage is along the +45° direction, as defined from the front (impacted side).

6. Comparison of apparent zones of damage as imaged by the polar backscatter technique (left panels) with photographs of damage indication from the deply technique (right panels). (a) -45° orientation: ILL 8. (b) 90° orinetation: ILL 9. (c) 0° orientation: ILL 12.

7. Correlation of damage areas estimated from the polar backscatter with corresponding damage areas derived from the deply technique.

8a. Backscatter signal from an undamaged region of the composite.

8b. System response measured as the backscattered wave from an aluminum block.

8c. Result of the Fourier deconvolution of figure 8a.

9a. Magnitude of the analytic function calculated from figure 8c. Identified are the front and back surface reflections and the lamina indications as noted.

9b. Magnitude of the analytic function for a backscattered wave in the damaged region of the composite.

10. Distribution of scattering amplitudes for an entire frame and a subsampled region which contains no damage.

11. Comparison of ultrasonic and deply techniques for the twelve possible interlaminar locations. (a) ultrasonic data frame.(b) photo of corresponding damage imaged by deply technique. (c) wire frame plot of part 'a' before frame is clipped.

12. Histogram comparison of ultrasonic and deply data for all four impact samples.

13. Correlation of ultrasonic and deply data. Line is a least square fit to the data and has correlation coefficent of 0.9.

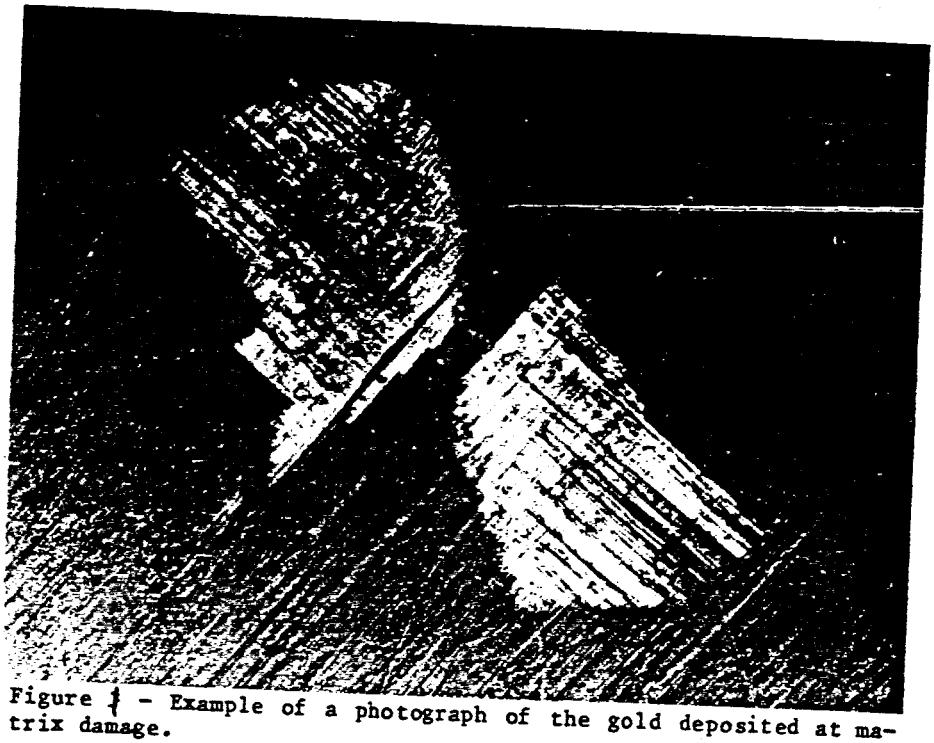

Figure 1 - Example of a photograph of the gold deposited at matrix damage.

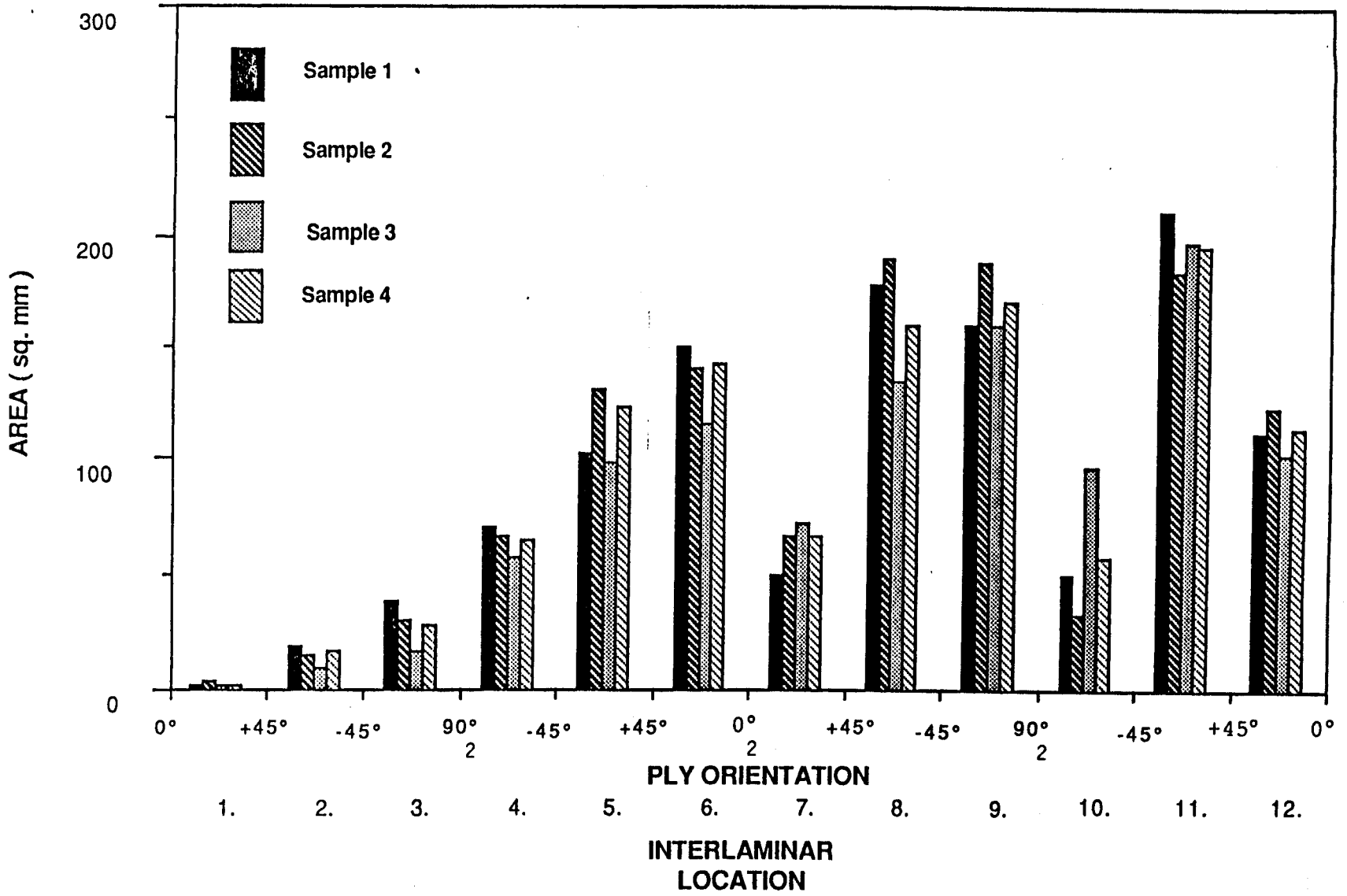
300
200
100
0
AREA (sq. mm)
Sample 1
Sample 2
Sample 3
Sample 4
0°
+45°
-45°
90°
2
-45°
+45°
0°
2
+45°
-45°
90°
2
-45°
+45°
0°
PLY ORIENTATION
1.
2.
3.
4.
5.
6.
7.
8.
9.
10.
11.
12.
INTERLAMINAR
LOCATION

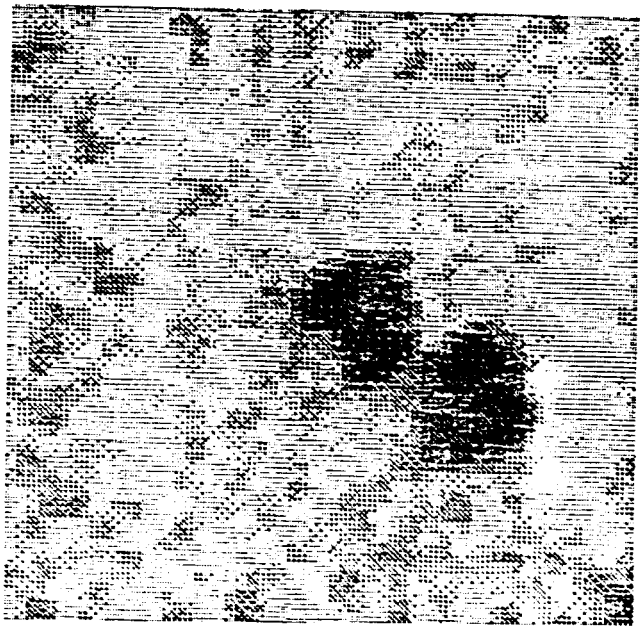

Figure 3 - Example of a gray scale image of a full 61 mm by 61 mm polar backscatter scan, interrogating perpendicular to the +45° orientation. The damage structure is oriented along the +45° direction.

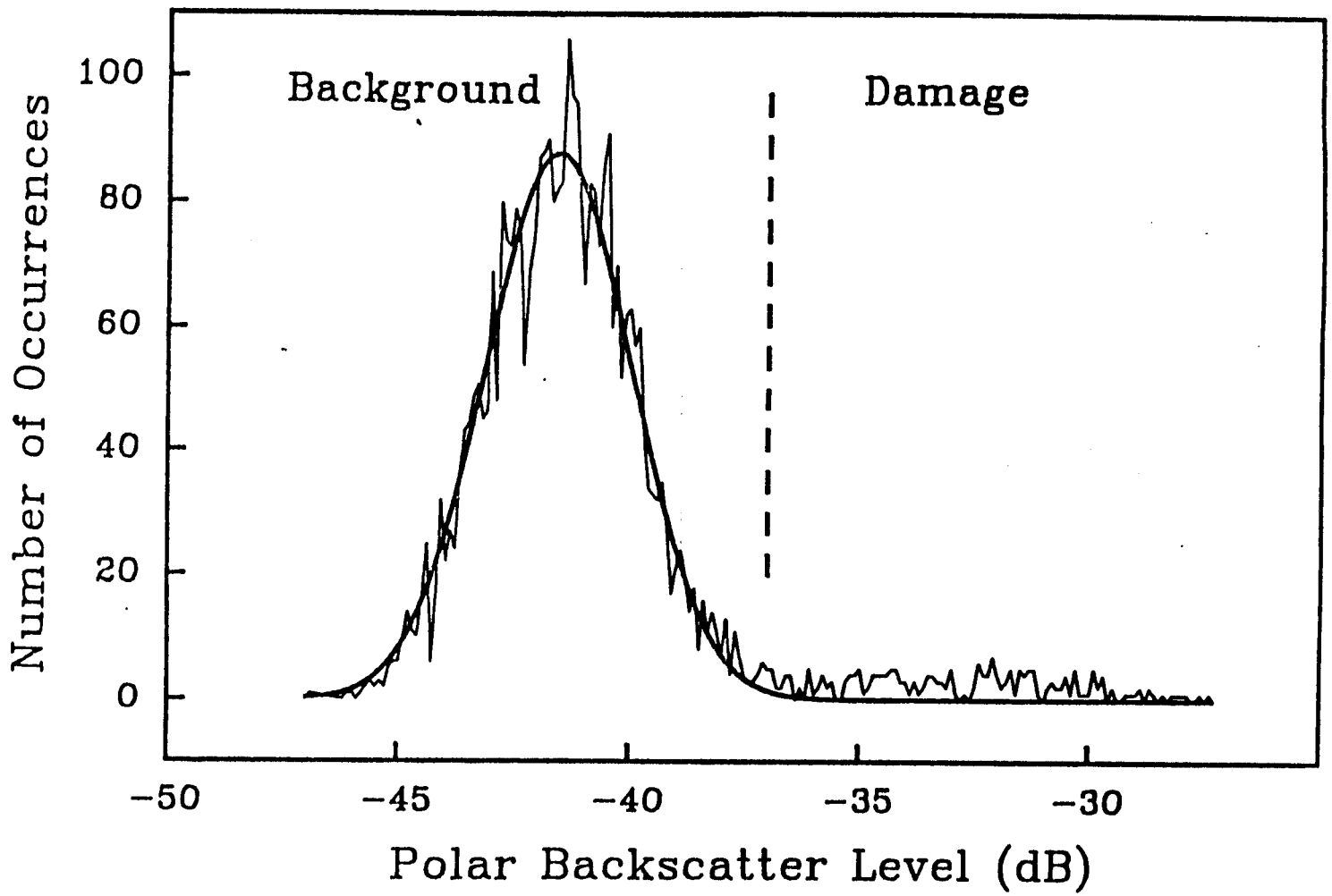
Background
Damage
Number of Occurrences
100
80
60
40
20
0
−50
−45
−40
−35
−30
Polar Backscatter Level (dB)

Polar Backscatter Image

Deply Photograph of Interlaminar Location 11-12

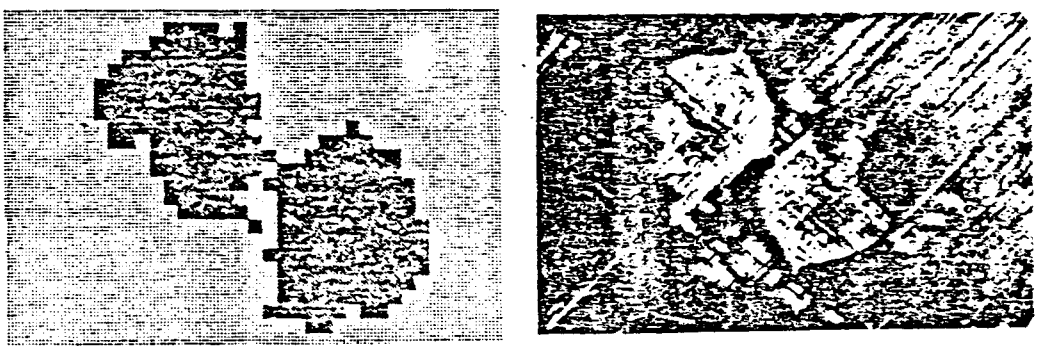

Figure 5 - Comparison of apparent zones of damage imaged by the polar backscatter technique (left panel) with photograph of damage indication from the deply technique. Orientation of the damage is along the $+45^{o}$ direction, as defined from the front (impacted) side.

Polar Backscatter Image

Deply Photographs

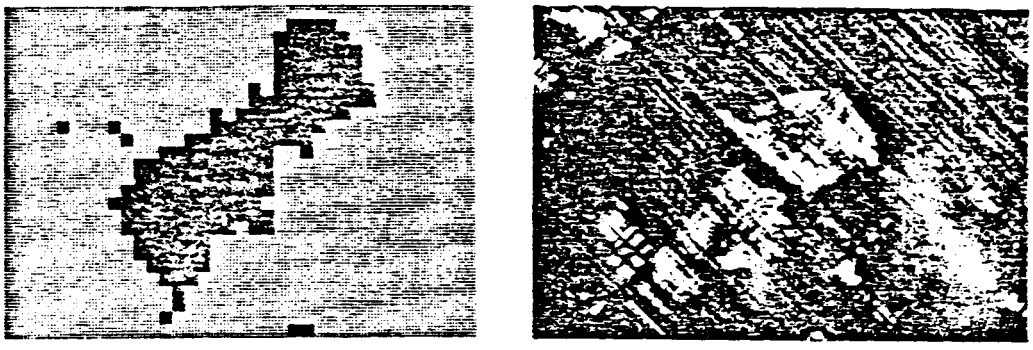

a) -45° orientation : Interlaminar Location 8-9

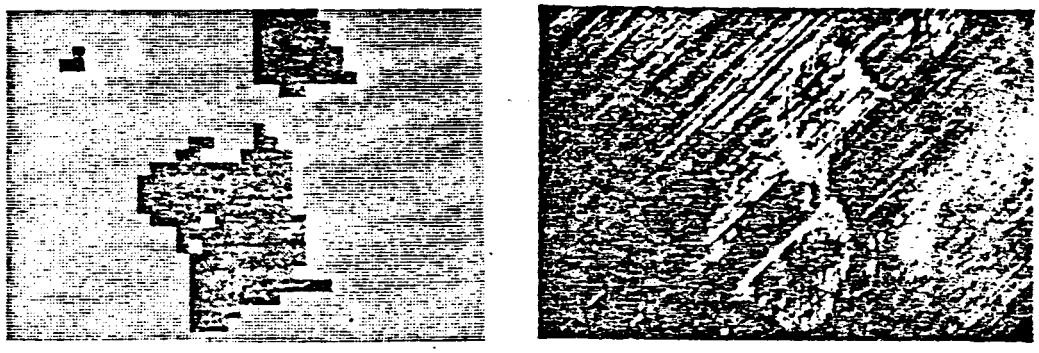

b) 90° orientation : Interlaminar Location 9-10

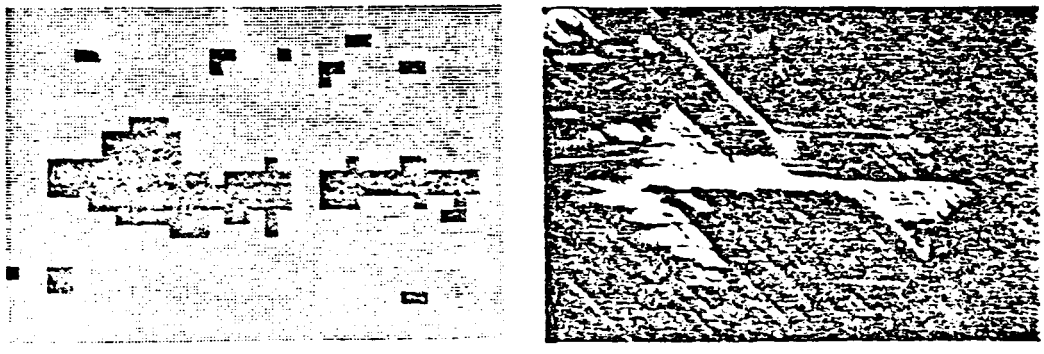

c) 0° orientation : Interlaminar Location 12-13

Figure 6 - Comparison of apparent zones of damage as imaged by the polar backscatter technique (left panels) with photographs of damage indication from the deply technique (right panels).

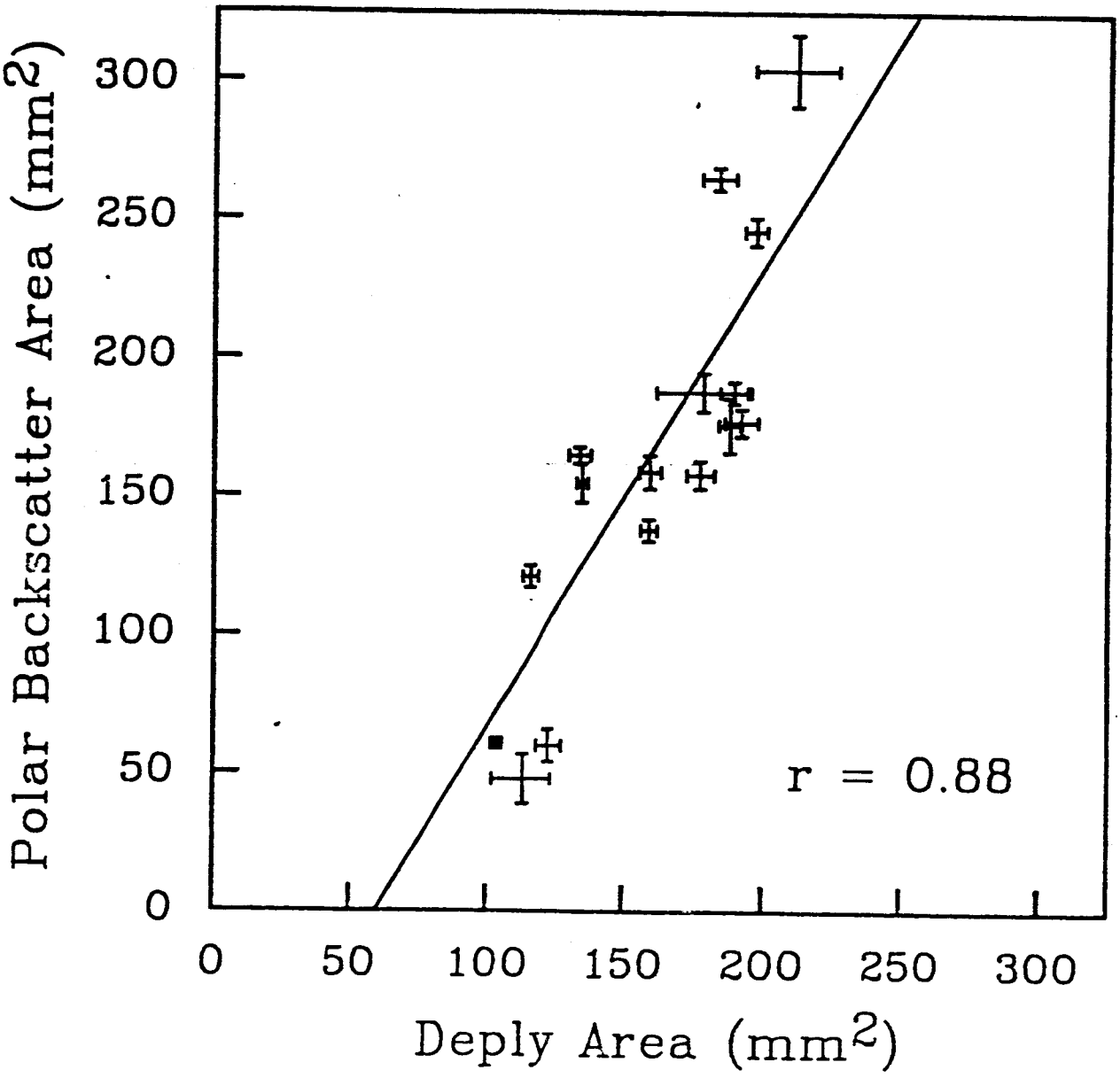
Polar Backscatter Area (mm2)
300
250
200
150
100
50
0
0
50
100
150
200
250
300
Deply Area (mm2)
r = 0.88

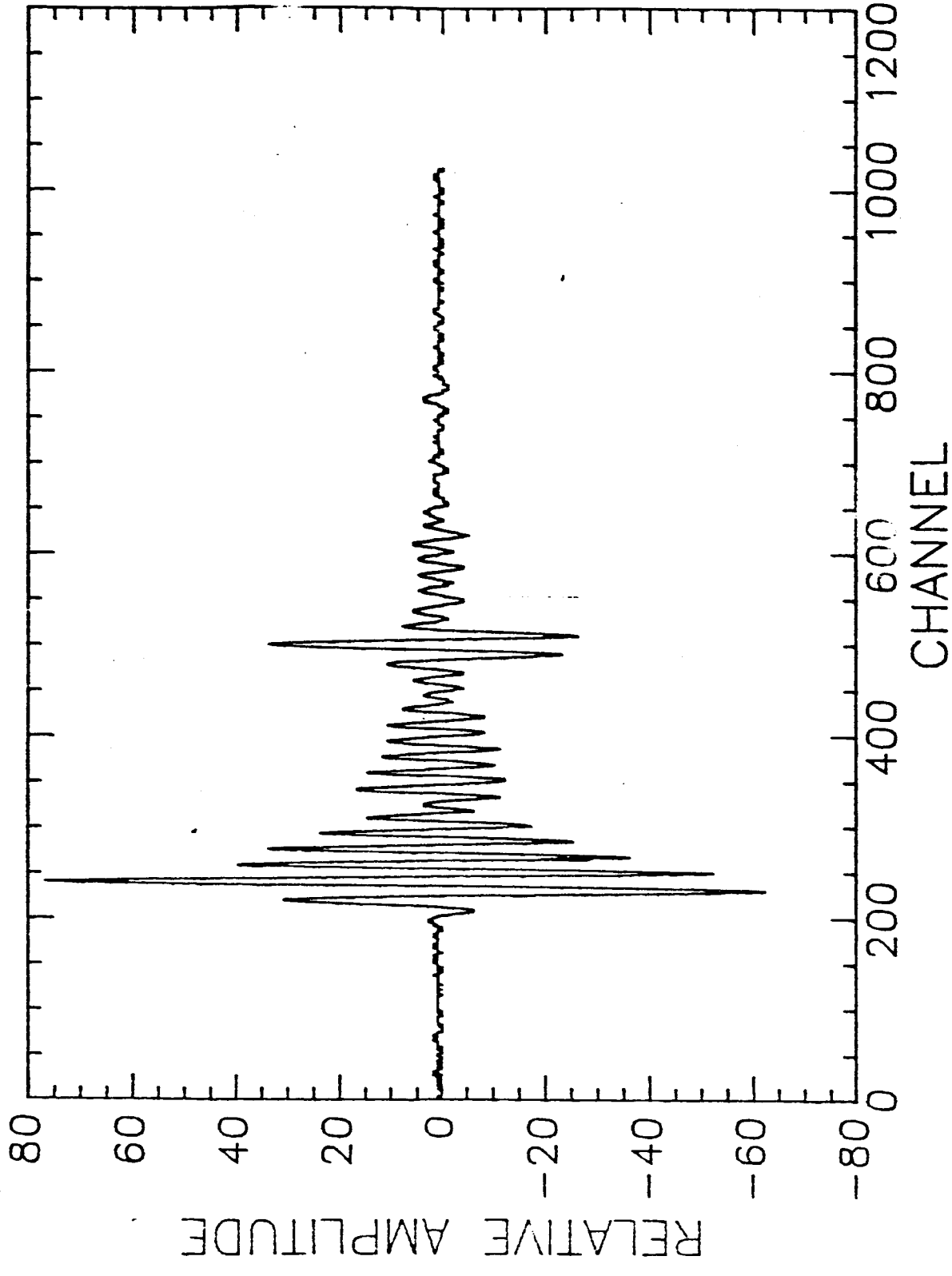
RELATIVE AMPLITUDE
80
60
40
20
0
-20
-40
-60
-80
0
200
400
600
800
1000
1200
CHANNEL

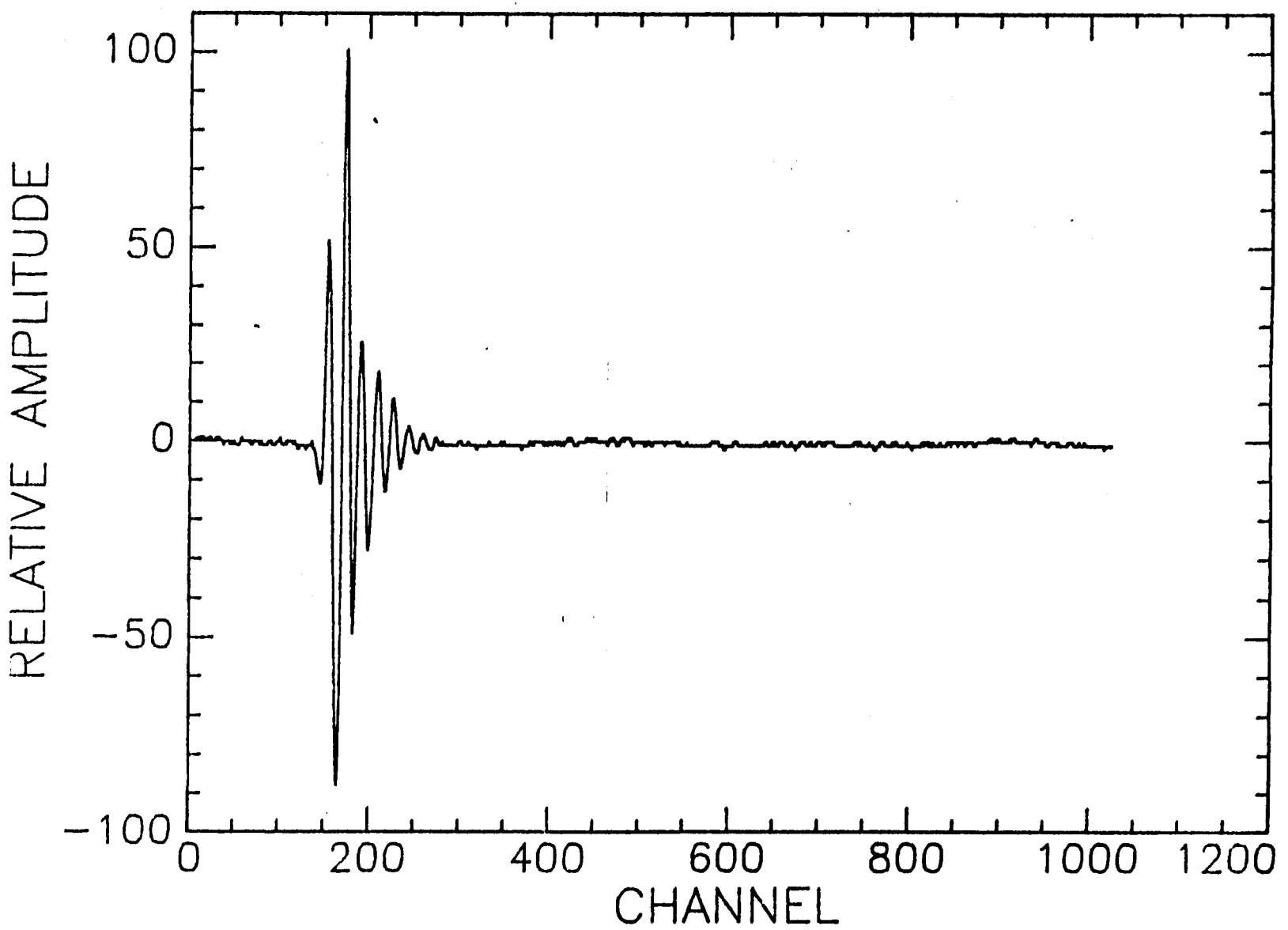
100
50
0
−50
−100
RELATIVE AMPLITUDE
0
200
400
600
800
1000
1200
CHANNEL

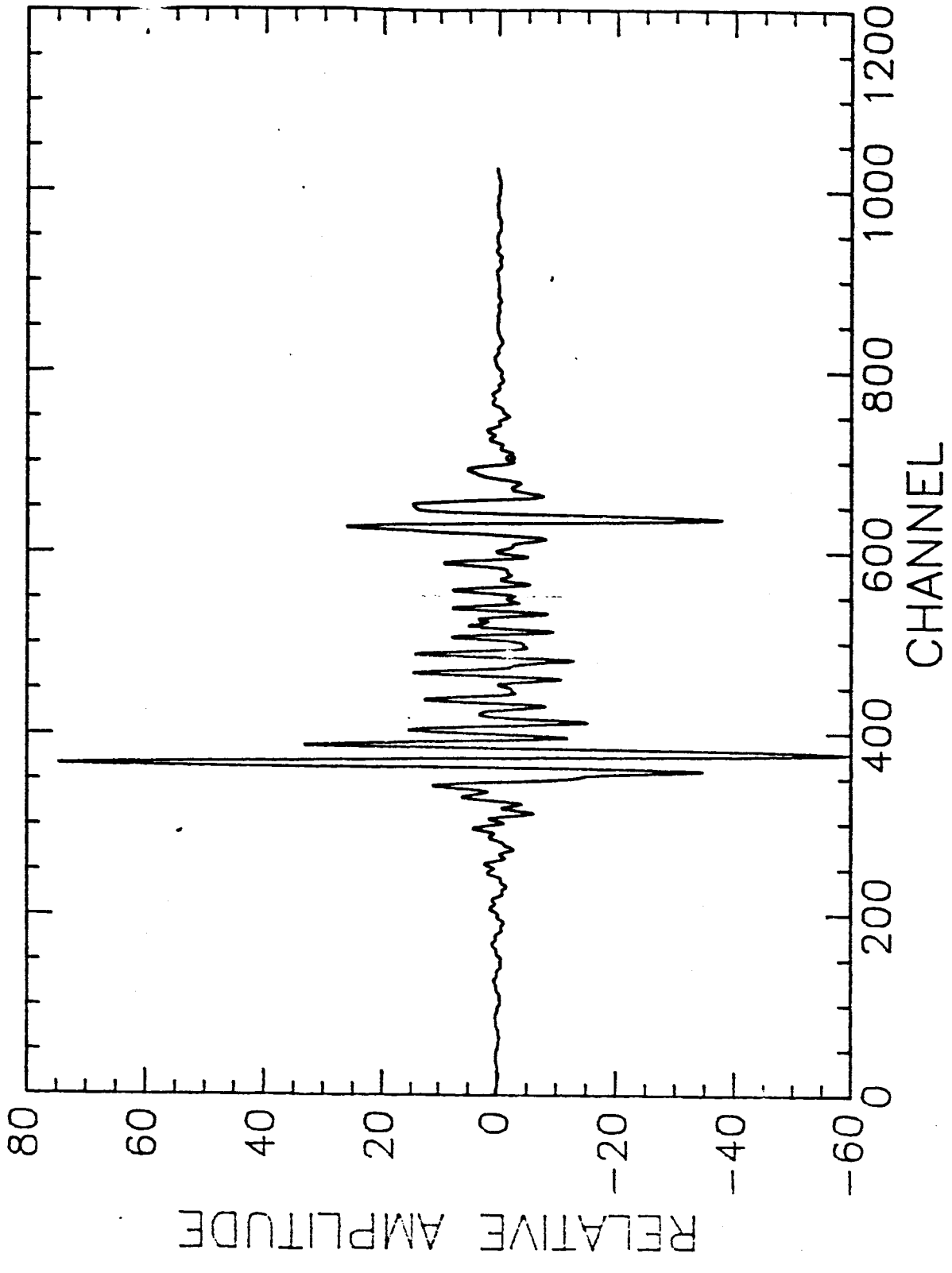
RELATIVE AMPLITUDE
80
60
40
20
0
-20
-40
-60
0
200
400
600
800
1000
1200
CHANNEL

8c.

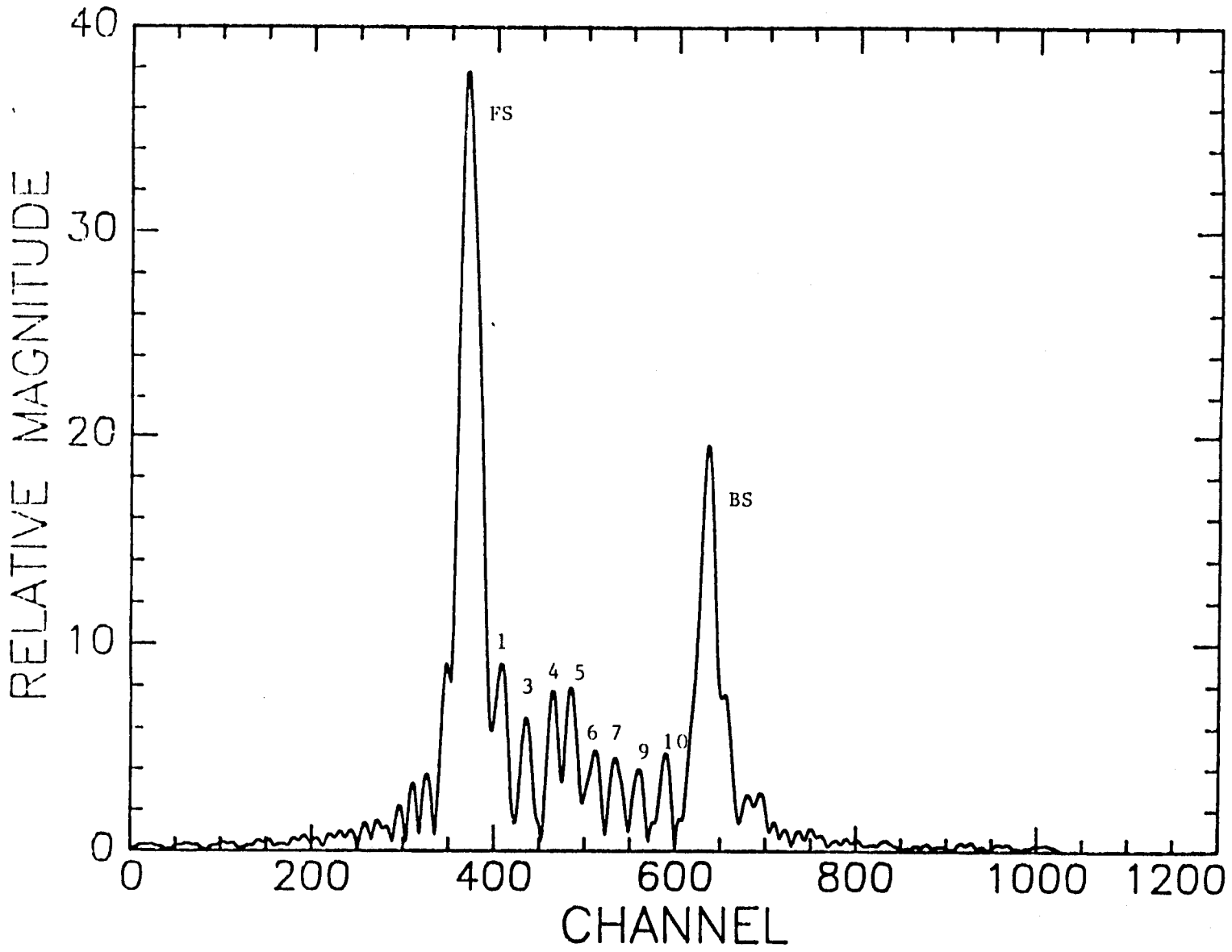
40
30
20
10
0
RELATIVE MAGNITUDE
FS
BS
1
3
4
5
6
7
9
10
0
200
400
600
800
1000
1200
CHANNEL

Figure 9a

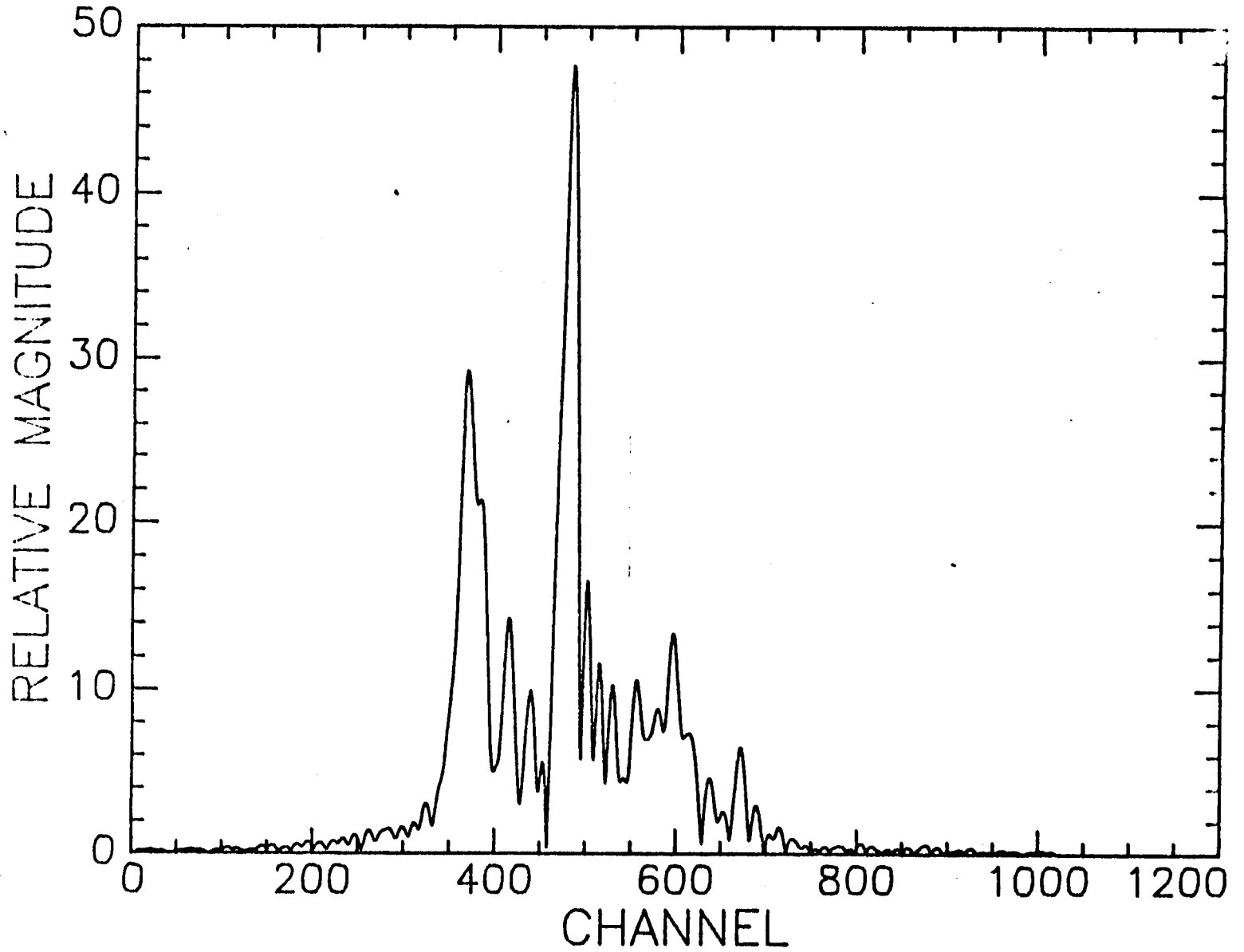
50
40
30
20
10
0
RELATIVE MAGNITUDE
0
200
400
600
800
1000
1200
CHANNEL

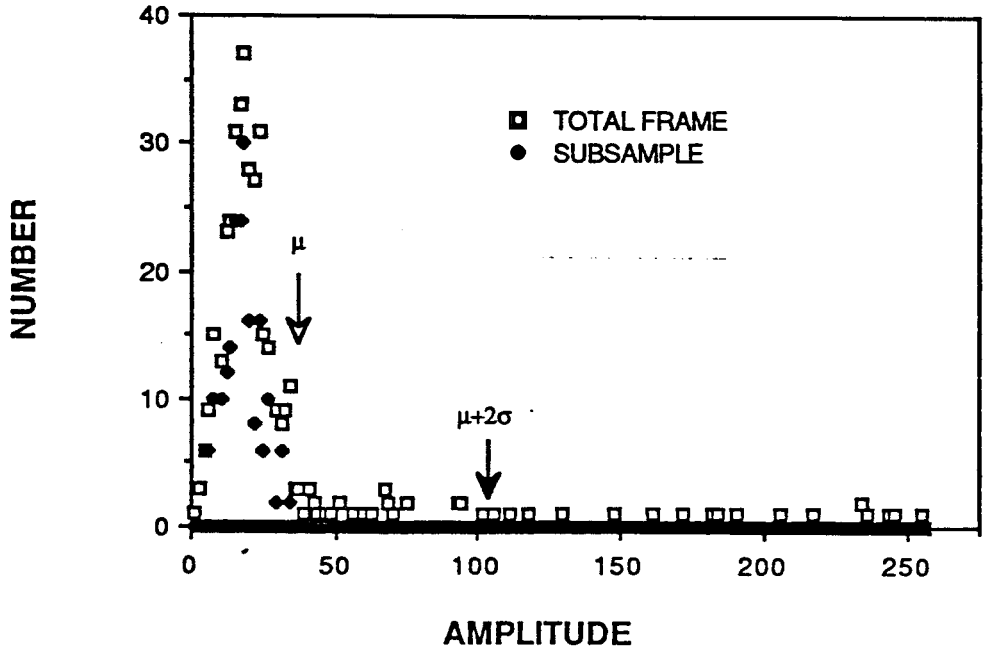
40
30
20
10
0
NUMBER
TOTAL FRAME
SUBSAMPLE
μ
μ+2σ
0
50
100
150
200
250
AMPLITUDE

ILL1

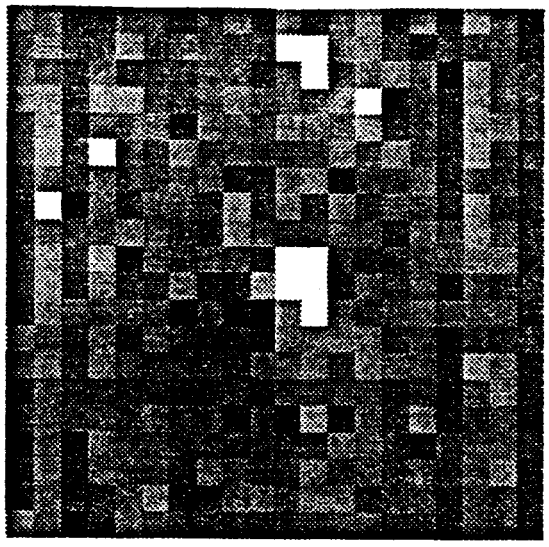

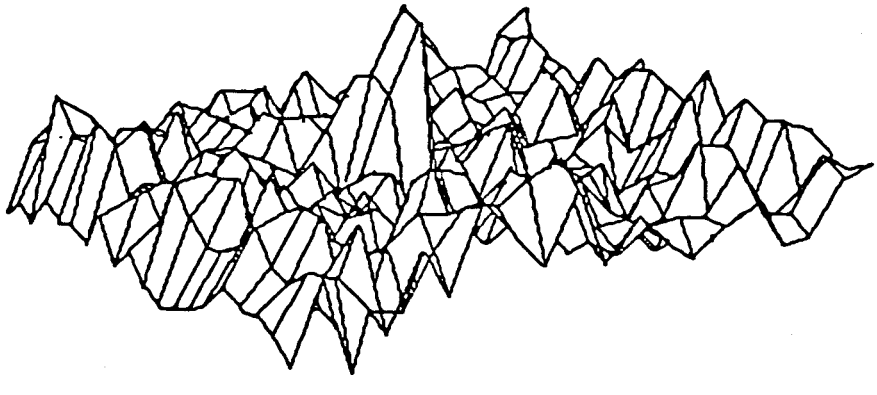

ILL2

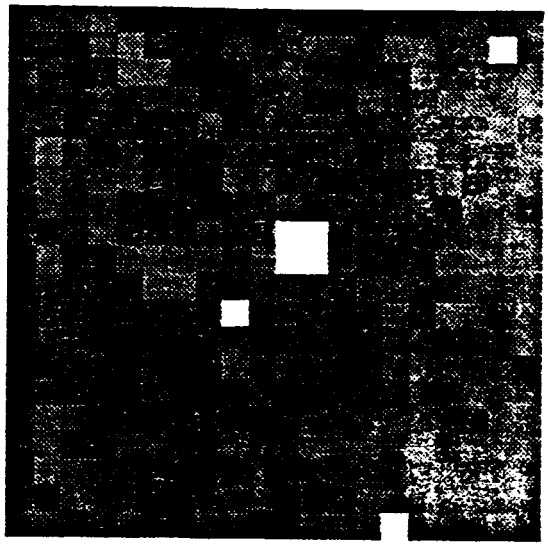

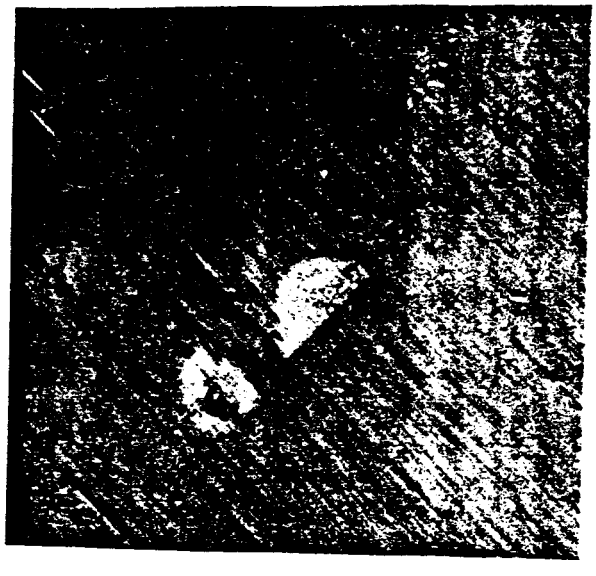

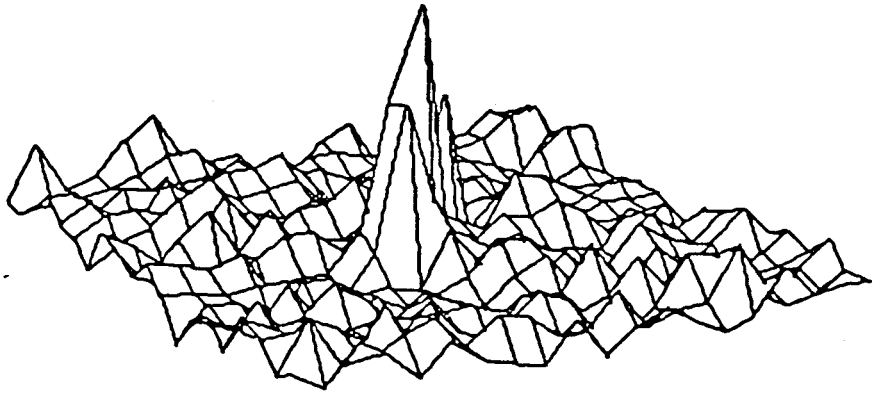

ILL3

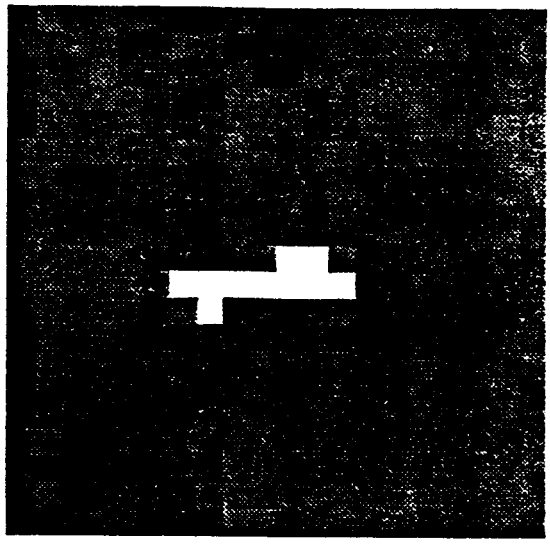

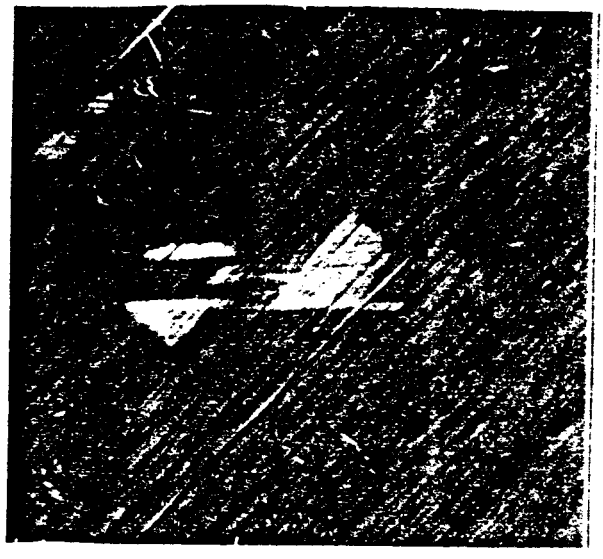

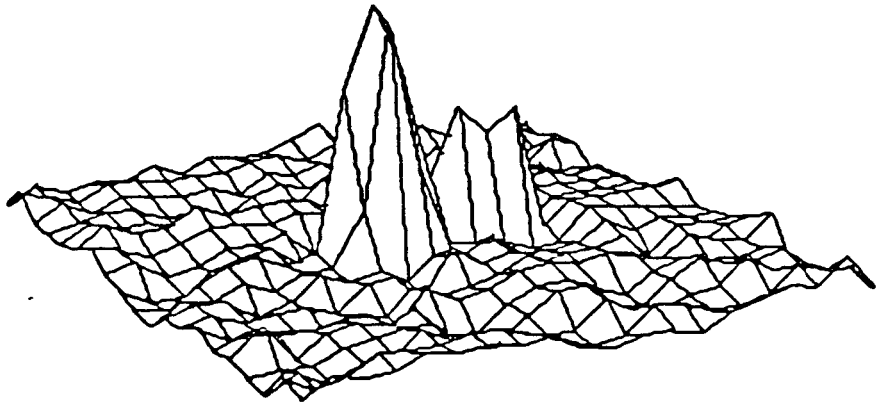

ILL4

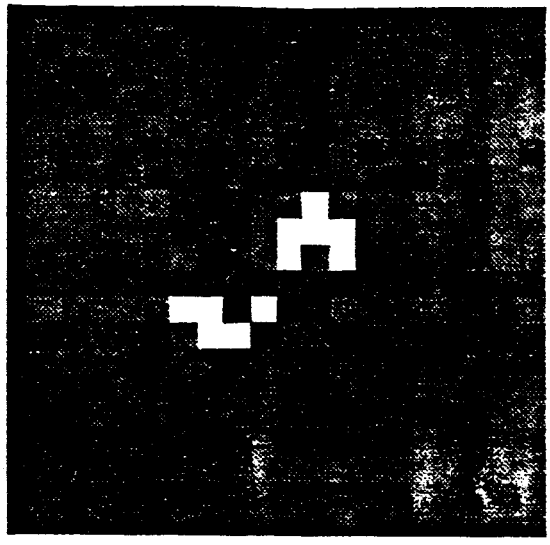

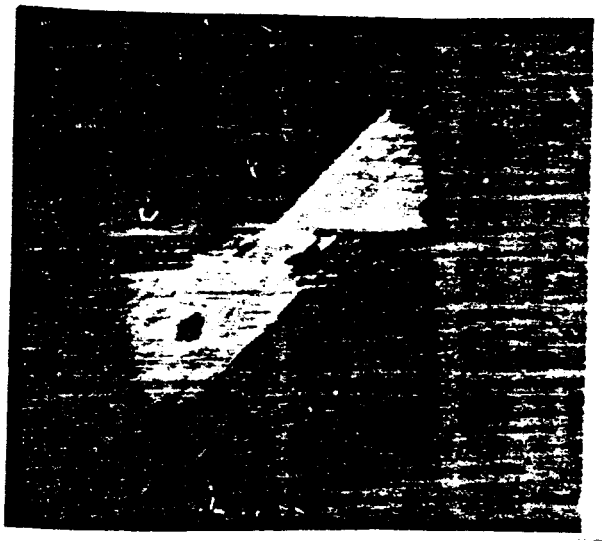

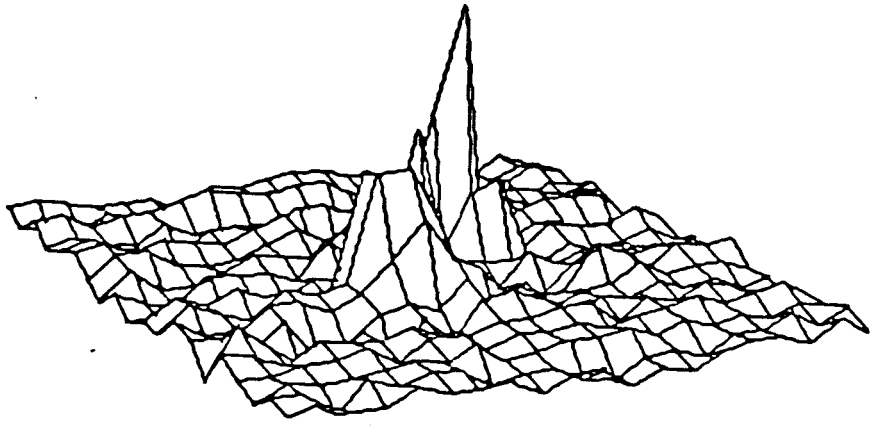

ILL5

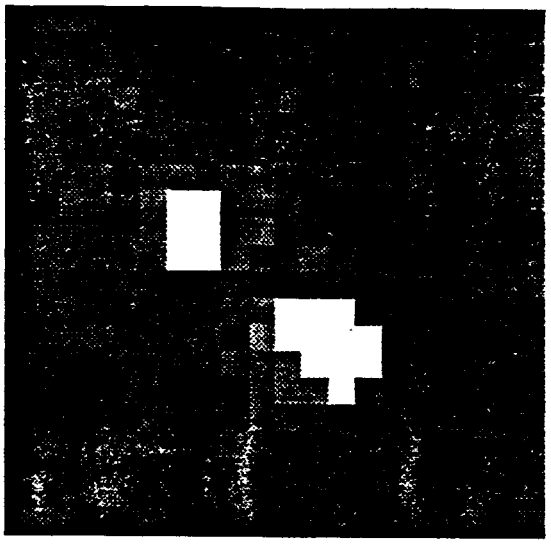

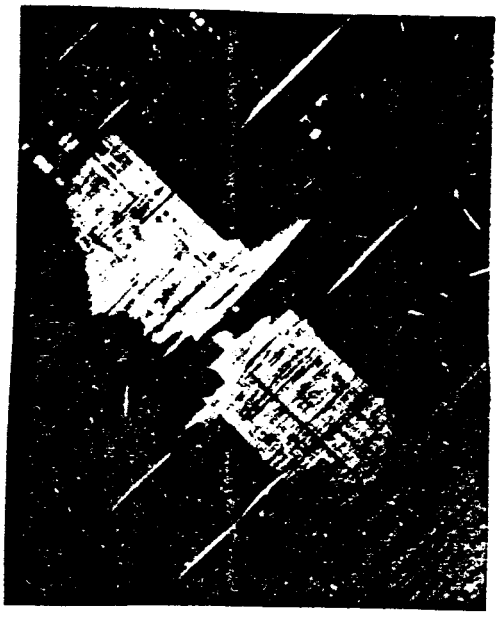

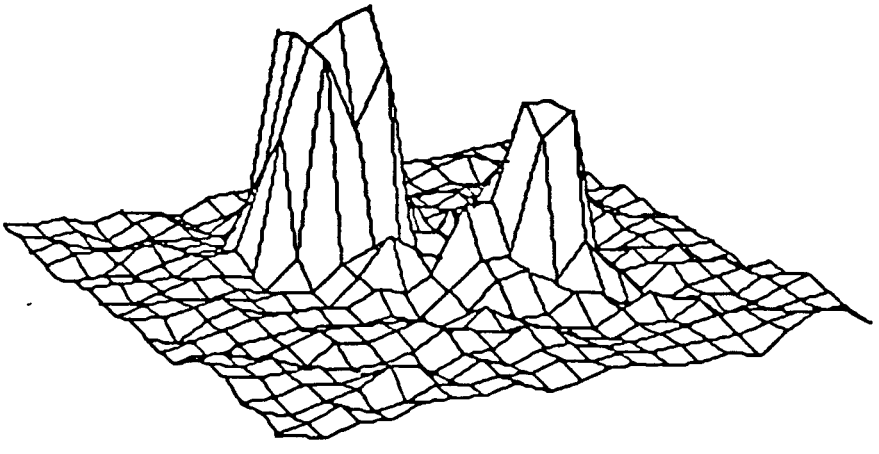

ILL6

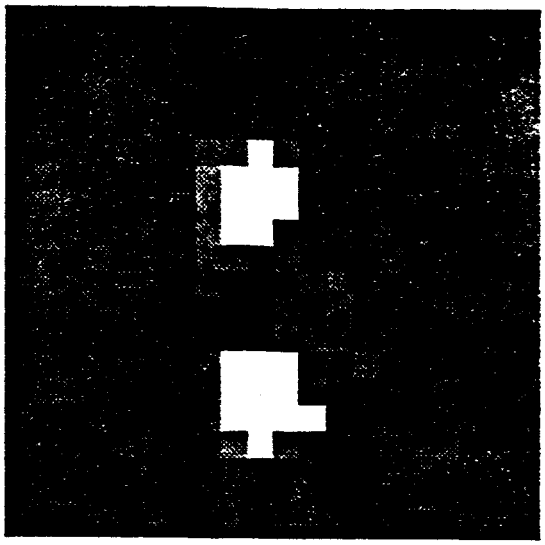

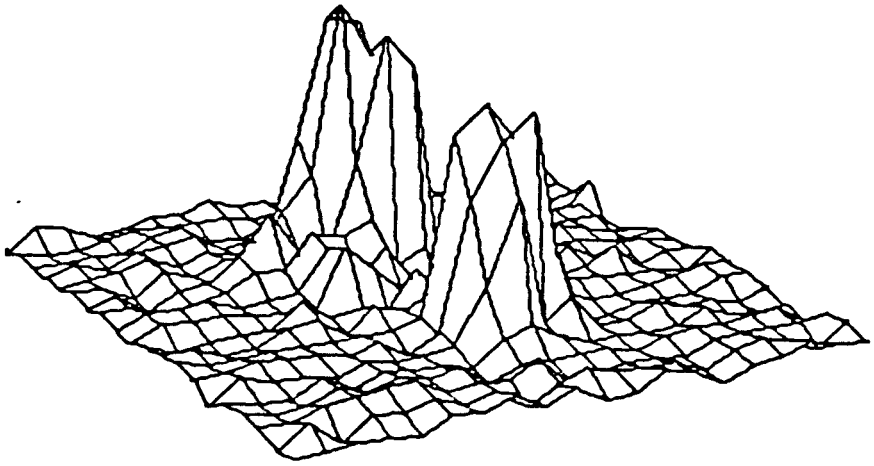

ILL7

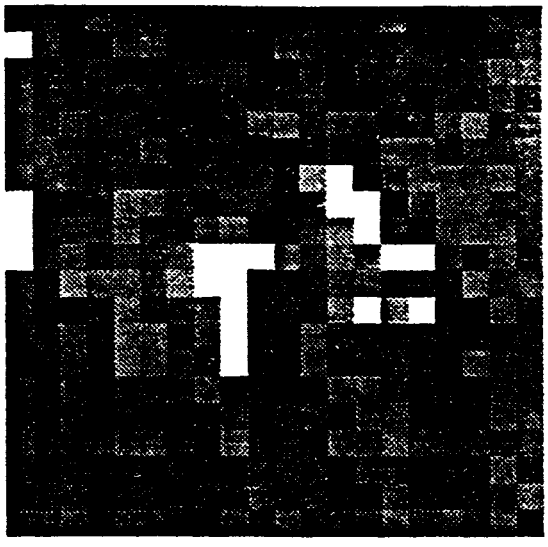

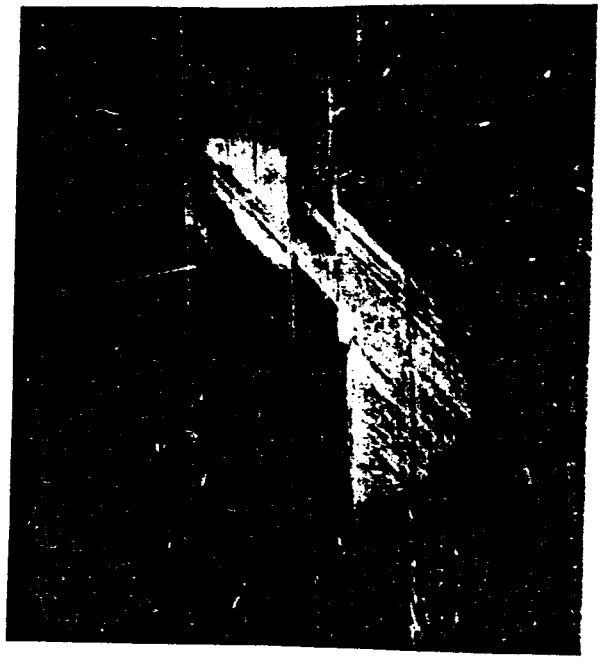

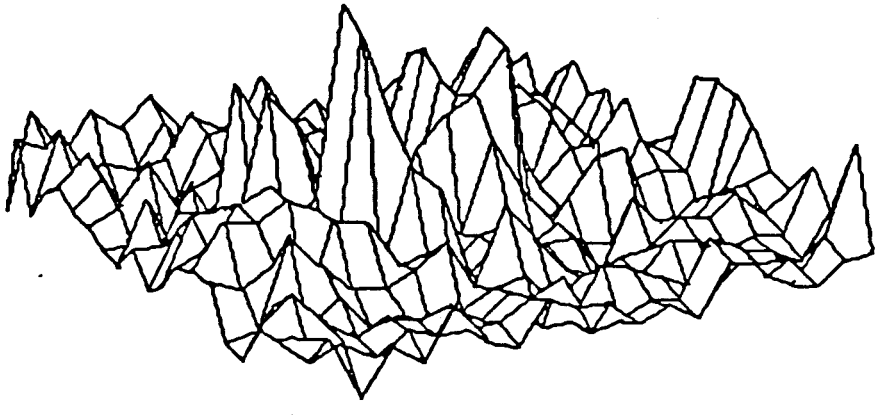

ILL8

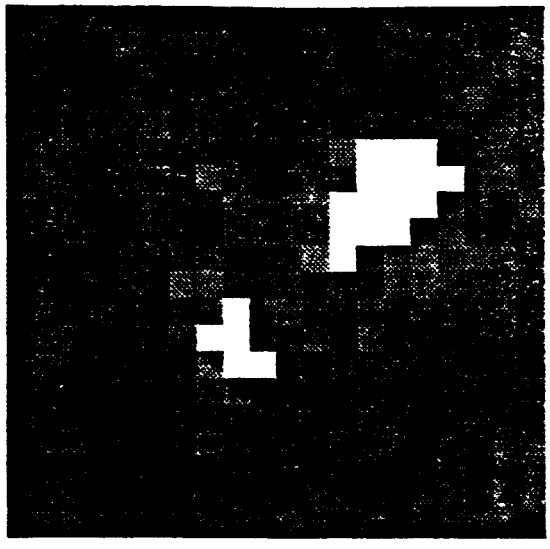

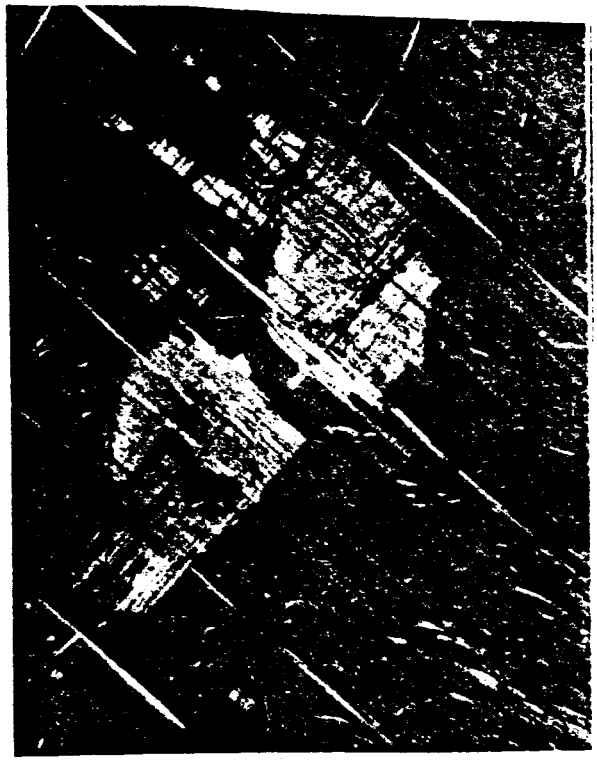

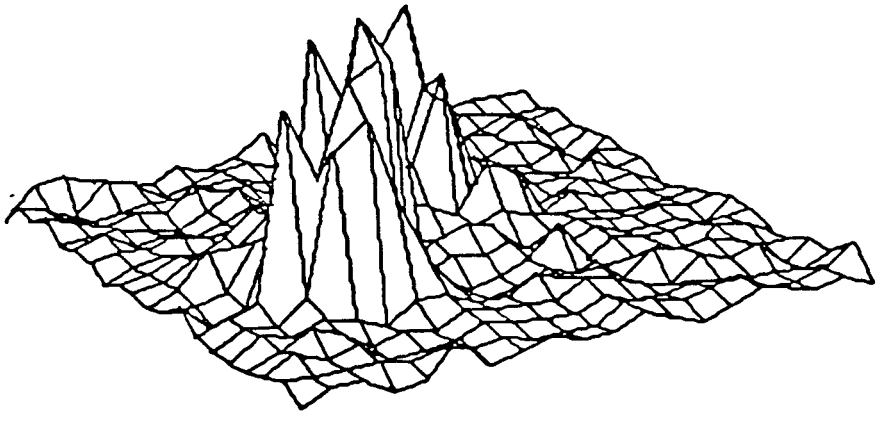

ILL9

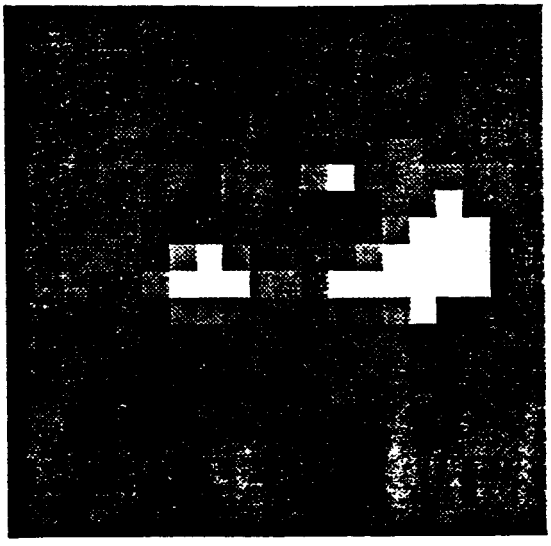

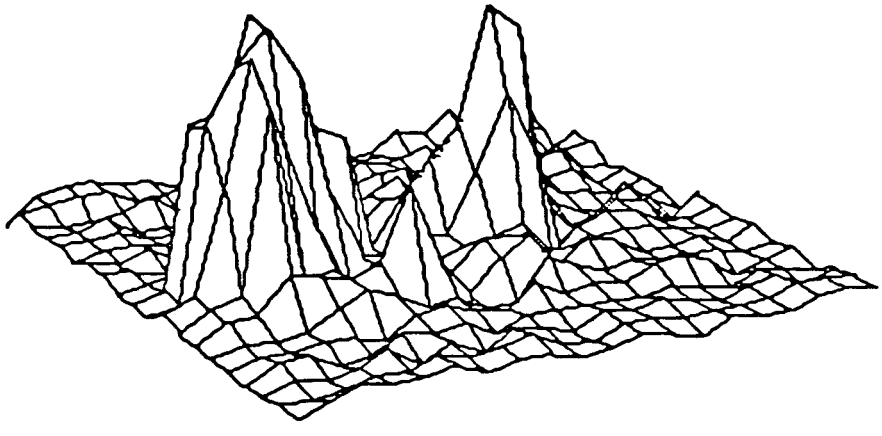

ILL10

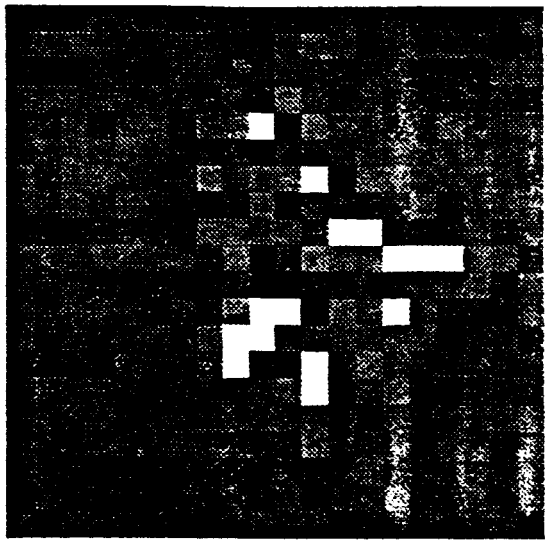

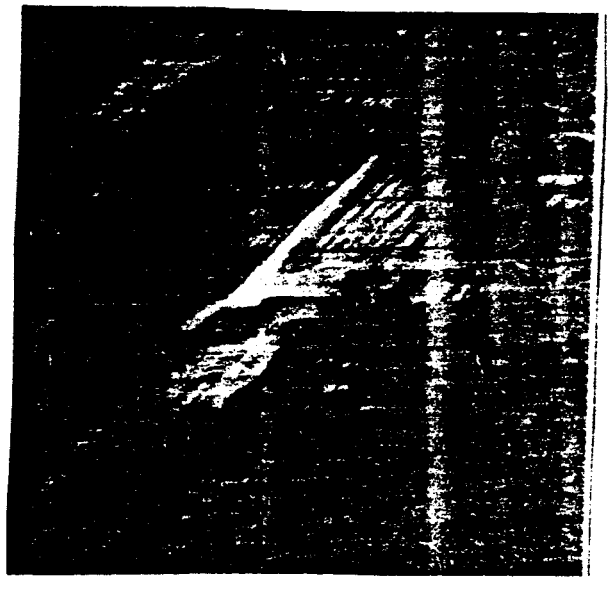

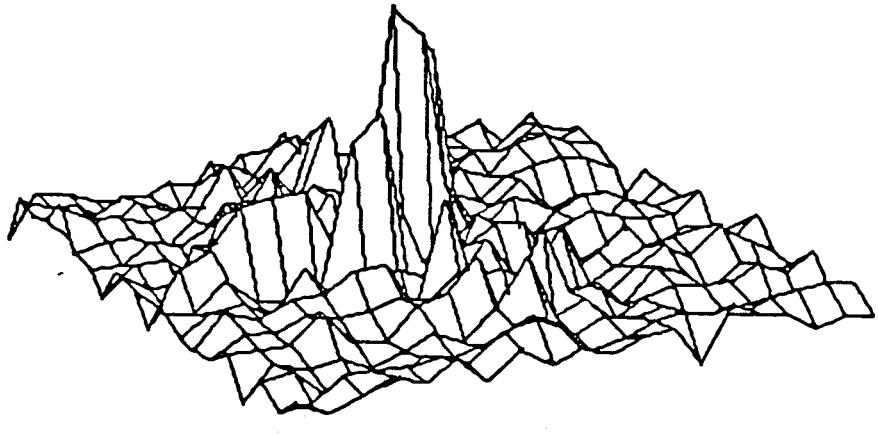

ILL11

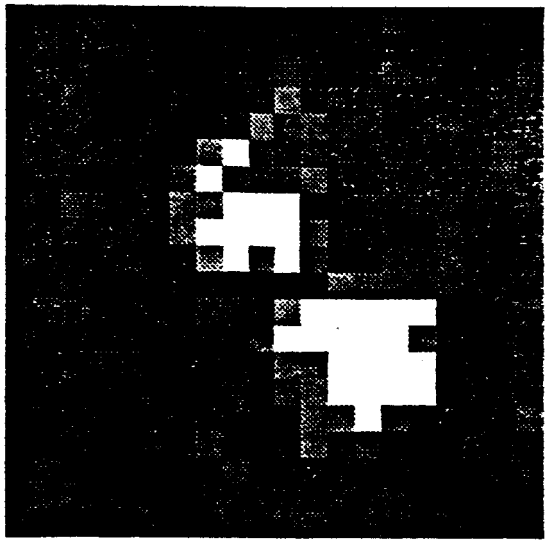

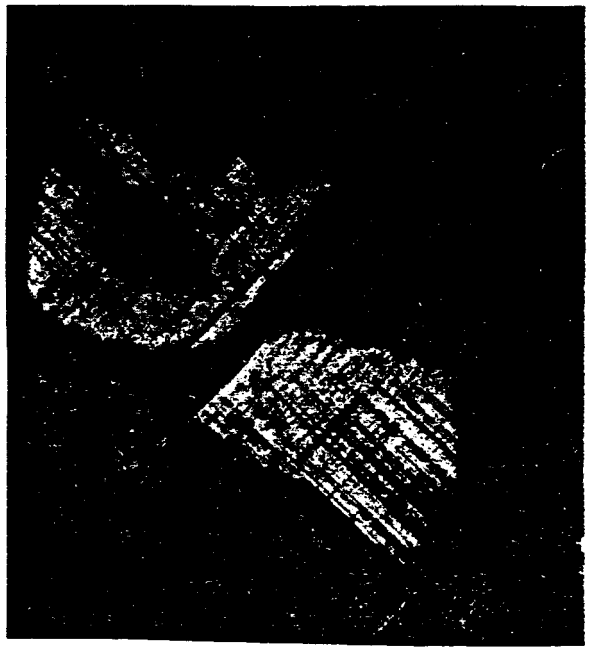

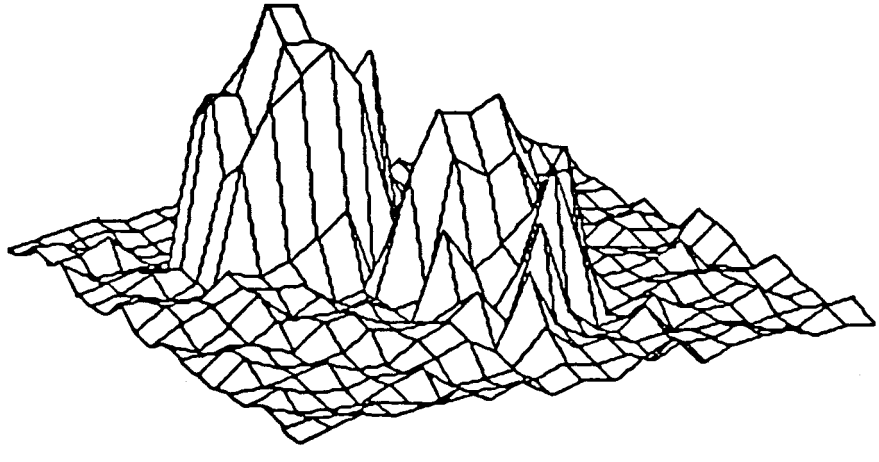

ILL12

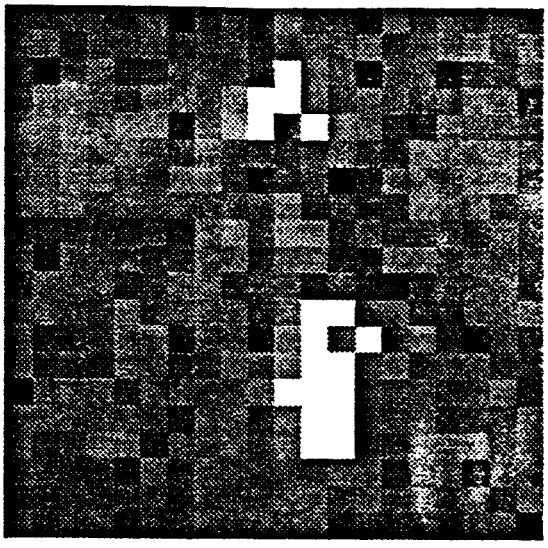

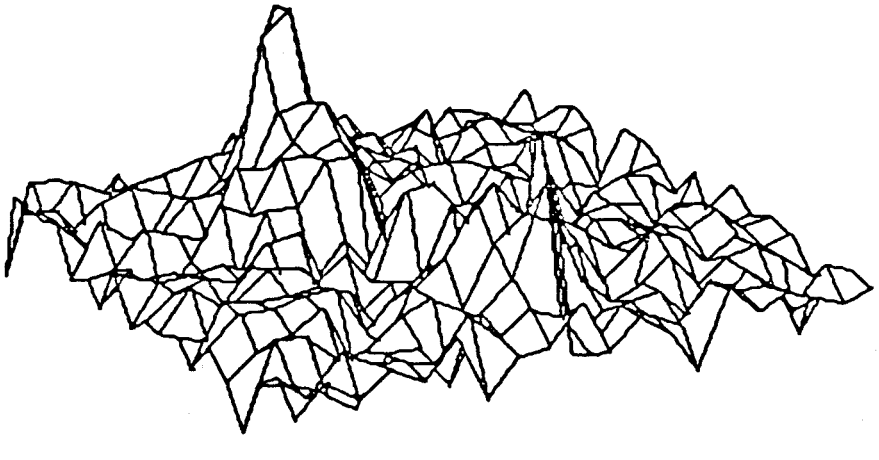

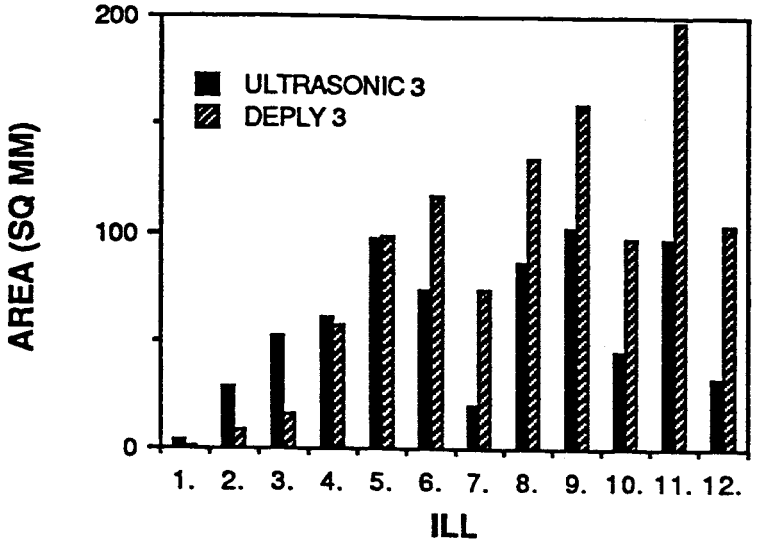
200
100
0
AREA (SQ MM)
ULTRASONIC 3
DEPLY 3
1. 2. 3. 4. 5. 6. 7. 8. 9. 10. 11. 12.
ILL

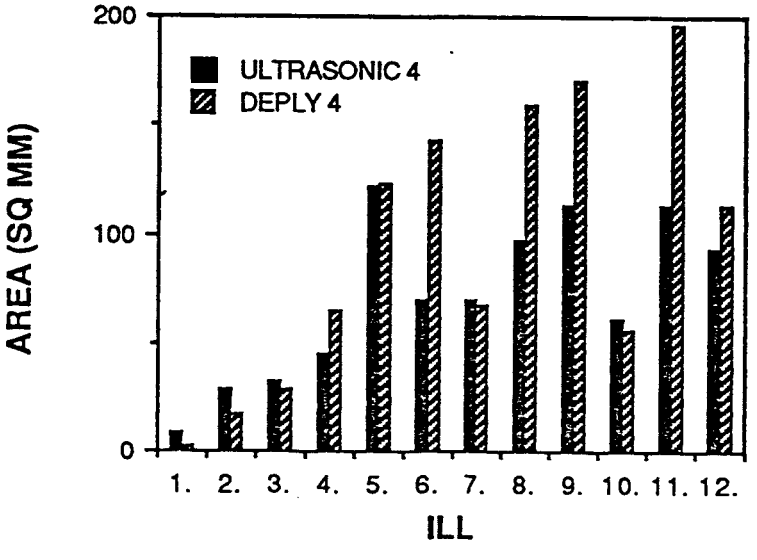
200
100
0
AREA (SQ MM)
ULTRASONIC 4
DEPLY 4
1. 2. 3. 4. 5. 6. 7. 8. 9. 10. 11. 12.
ILL

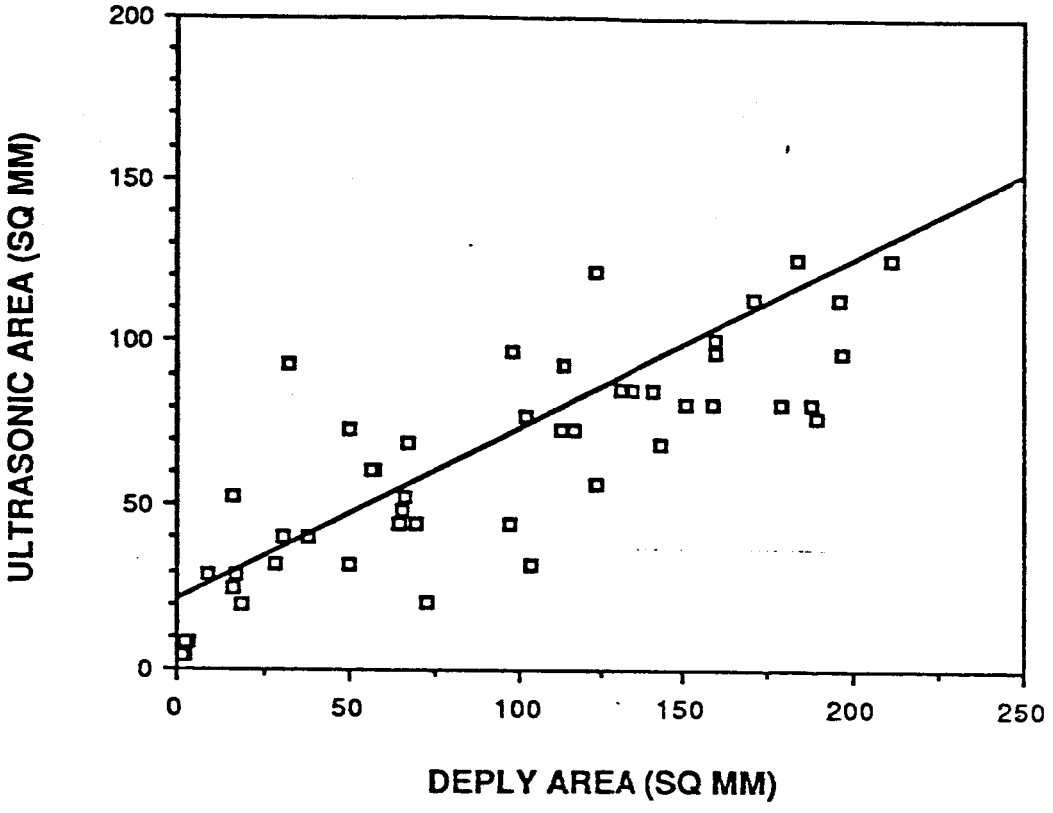
ULTRASONIC AREA (SQ MM)
200
150
100
50
0
0
50
100
150
200
250
DEPLY AREA (SQ MM)